nature communications

Article

https://doi.org/10.1038/s41467-025-60475-0

Methionine cycle in *C. elegans* serotonergic neurons regulates diet-dependent behaviour and longevity through neuron-gut signaling

Received: 6 February 2024

Accepted: 27 May 2025

Published online: 02 June 2025

Check for updates

Sabnam Sahin Rahman[1], Shreya Bhattacharjee[1], Simran Motwani[1], Govind Prakash[1], Rajat Ujjainiya[2,3], Shivani Chitkara[3], Tripti Nair[1,4], Rachamadugu Sai Keerthana[1], Shantanu Sengupta[2,3] & Arnab Mukhopadhyay[1]

The folate and methionine cycles (Met-C) are regulated by vitamin B12 (B12), obtained exclusively from diet and microbiota. Met-C supports amino acid, nucleotide, and lipid biosynthesis and provides one-carbon moieties for methylation reactions. While B12 deficiency and polymorphisms in Met-C genes are clinically attributed to neurological and metabolic disorders, less is known about their cell-non-autonomous regulation of systemic physiological processes. Using a B12-sensitive *Caenorhabditis elegans* mutant, we show that the neuronal Met-C responds to differential B12 content in diet to regulate p38-MAPK activation in the intestine, thereby modulating cytoprotective gene expression, osmotic stress tolerance, behaviour and longevity. Mechanistically, our data suggest that B12-driven changes in the metabolic flux through the Met-C in the mutant's serotonergic neurons increase serotonin biosynthesis. Serotonin activates its receptor, MOD-1, in the post-synaptic interneurons, which then secretes the neuropeptide FLR-2. FLR-2 binding to its intestinal receptor, FSHR-1, induces the phase transition of the SARM domain protein TIR-1, thereby activating the p38-MAPK pathway. Together, we reveal a dynamic neuron-gut signalling axis that helps an organism modulate life history traits based on the status of neuronal Met-C, determined by B12 availability in its diet.

Animals depend on dietary sources and their microbiota for the supply of B12[1,2]. B12 exists in two biologically active forms, methylcobalamin and adenosylcobalamin, functioning as coenzymes for cytosolic methionine synthase (MS) and mitochondrial methylmalonyl-CoA mutase, respectively. MS joins the cytosolic folate cycle and the methionine cycle (Met-C), facilitating the transfer of methyl group from methyltetrahydrofolate to homocysteine, resulting in the formation of methionine (Fig. 1A)[3]. Methionine, in conjunction with ATP, undergoes further conversion to S-adenosylmethionine (SAM). SAM, in turn, serves as the primary methyl donor for the methylation of DNA, RNA or other cellular metabolites, and is converted to S-adenosyl homocysteine (SAH). Met-C also supplies key metabolites for the biosynthesis of amino acids, nucleotides, and lipids[4,5]. Thus, B12 deficiency leads to increased susceptibility to disorders like depression, anxiety, and schizophrenia while polymorphism in the genes of the Met-C is linked to increased risk of obesity, insulin resistance, cardiovascular disease, and cancer[2,6–11]. However, the precise mechanisms underpinning the association between B12 deficiency, Met-C gene

[1]Molecular Aging Laboratory, BRIC-National Institute of Immunology, Aruna Asaf Ali Marg, New Delhi, India. [2]CSIR-Institute of Genomics and Integrative Biology, New Delhi, India. [3]Academy of Scientific and Innovative Research (AcSIR), Ghaziabad, India. [4]Present address: Leonard Davis School of Gerontology, University of Southern California, Los Angeles, CA, USA. e-mail: arnab@nii.ac.in

https://doi.org/10.1038/s41467-025-60475-0

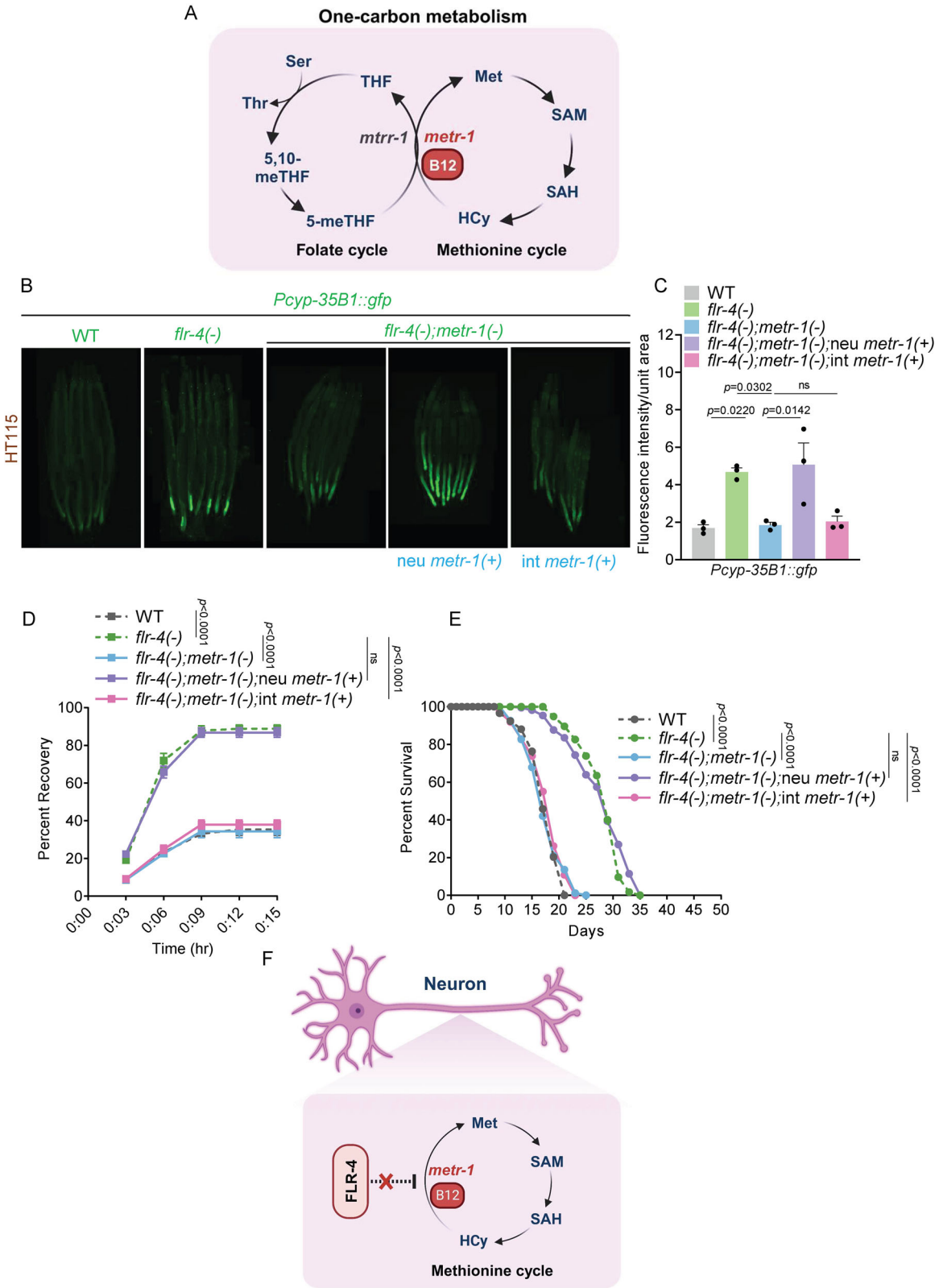

polymorphism and their pathological outcomes are not fully understood. Importantly, whether and how B12-driven changes in Met-C in one tissue may affect systemic physiology through effects on a distal tissue is less known.

In vertebrates, two distinct mechanisms are involved in the remethylation of homocysteine to methionine, one catalyzed by the B12-dependent MS, and other by a vitamin B6-depedent betaine-homocysteine methyltransferase (BHMT)[12]. Like other invertebrates, *Caenorhabditis elegans* lacks BHMT and depends entirely on MS. In spite of these differences, this nematode plays a prominent role in our efforts to understand the contributions of B12 and Met-C in cellular physiology, highlighting the importance of host-microbiota interactions on a spectrum of life-history traits, gene expression dynamics, and metabolic adaptations[13–17]. *C. elegans* is a bacterivore that feeds on diverse bacterial

Fig. 1 | Met-C in the neuron modulates CyTP gene expression, osmotic stress tolerance and lifespan of *flr-4(n2259)*. **A** A schematic representation of the folate and methionine cycle (Met-C) in *Caenorhabditis elegans*. Created in BioRender. Mukhopadhyay, A. (2025) https://BioRender.com/83r2ngb. **B** The expression of *gfp* in *flr-4(n2259);metr-1(ok521);Pcyp35B1::gfp* worms was restored when *metr-1* was rescued only in the neurons (using the pan-neuronal *rgef-1* promoter) [neu *metr-1(+)*] but not when rescued in the intestine (using the *ges-1* promoter) [int *metr-1(+)*]. One of three biologically independent replicates is shown. **C** Quantification of (**B**). Average of three biological replicates ± SEM. *P*-value determined using One-way ANOVA with Tukey's multiple comparisons test. $P \geq 0.05$ was considered not significant, ns. **D** The osmotic stress tolerance of *flr-4(n2259);metr-1(ok521)* worms were restored when *metr-1* was rescued only in the neurons (using the pan-neuronal *rgef-1* promoter) [neu *metr-1(+)*] but not when rescued in the intestine (using the *ges-1* promoter) [int *metr-1(+)*]. One of three biologically independent replicates is shown. *P*-value was determined using Two-way ANOVA with Tukey's multiple comparisons test. $P \geq 0.05$ was considered not significant, ns. **E** The lifespan of *flr-4(n2259);metr-1(ok521)* worms were restored when *metr-1* was rescued only in the neurons (using the pan-neuronal *rgef-1* promoter) [neu *metr-1(+)*] but not when rescued in the intestine (using the *ges-1* promoter) [int *metr-1(+)*]. One of three biologically independent replicates is shown. *P*-value was determined using Mantel–Cox log-rank test. $P \geq 0.05$ was considered not significant, ns. **F** A schematic illustrating that the Met-C is required in the neurons for *flr-4(n2259)* phenotypes. Created in BioRender. Mukhopadhyay, A. (2025) https://BioRender.com/83r2ngb. All experiments were performed at 20 °C. All data and analysis are provided in the Source Data file.

species in both its natural habitats and in controlled laboratory settings; thus, bacteria act both as food and the microbiota of the worms. So, like mammals, the worms are entirely dependent on their bacterial diet for B12 supply. Additionally, due to the availability of diverse genetic, biochemical and cell biology tools, it serves as a popular model system for the exploration of inter-tissue crosstalk in evolutionarily conserved cellular pathways regulating stress responses, diseases, and aging[18–20].

To study the effects of B12 on systemic physiology, a sensitized genetic background is necessary. This is because the wild-type worms that feed on a wide range of bacterial diets, can maintain cellular and metabolic homeostasis orchestrated by specific genes, preventing alteration of life-history traits on different diets rich in diverse nutrients[21]. However, occasionally we come across genetic mutants that show altered life-history traits specific to one diet and not others. These 'gene-diet pairs' have significantly contributed to our knowledge of the impact of food quality and microbiota on both lifespan and health[22]. Our laboratory has characterized one such diet-gene pair where a serine-threonine kinase gene (*fluoride resistance 4* or *flr-4*) mutant displays an increased sensitivity to B12 and exhibits enhanced cytoprotective gene (CyTP) expression, osmotic stress tolerance, and lifespan only on the B12-rich *E. coli* HT115 but not on *E. coli* OP50[23,24], providing us with the perfect paradigm to study the regulation of Met-C by B12 and its effect on organismal physiology.

When the kinase-dead allele *flr-4(n2259)* [referred to as *flr-4(-)*] is fed HT115 or OP50 supplemented with B12, the metabolic flux through the Met-C cycle is augmented, leading to the downstream activation of the p38-MAPK pathway[24]. Notably, *flr-4* is expressed both in the neurons as well as the intestine[23], suggesting that the gene may independently affect the Met-C and the p38-MAPK pathway in distinct tissues. Here, we show that metabolically active bacteria provide both B12 and the essential amino acid methionine to the host. The B12- and methionine-driven changes in Met-C take place in the serotonergic ADF neurons of *flr-4(-)* while the p38-MAPK is activated in the intestine. 5-HT secreted from these neurons engages its cognate receptor MOD-1 in the post-synaptic interneuron, which then releases the glycoprotein hormone/neuropeptide FLR-2. FLR-2 activates its receptor in the intestinal cells and directs the phase transition of the SARM domain-containing TIR-1 protein, which in turn activates the p38-MAPK pathway. This results in an increase in CyTP gene expression, osmotic stress tolerance, and longevity in *flr-4(-)* worms. Importantly, this axis also regulates the foraging behavior of the mutant, directing them toward the B12-rich diet. Together, our study elucidates a novel neuron-gut signaling cascade that transmits the information of neuronal Met-C to modulate gene expression in the distal intestinal cells to regulate lifespan in response to a diet of varying B12 content.

Results

The neuronal Met-C is essential for CyTP gene expression, osmotic stress tolerance, and longevity of the *flr-4* mutant

In our previous study, we demonstrated that the *flr-4(-)* worms exhibit increased health span and lifespan when grown on a B12-rich diet such as HT115 or OP50 supplemented with B12[24]. Feeding a B12-rich diet to the *flr-4(-)* increases the tissue concentrations of the micronutrient (Supplementary Fig. S1A) and methionine (Supplementary Fig. S1B, C). To evaluate whether the phenotypic benefits of a B12-rich diet in *flr-4(-)* require metabolically active bacteria, we utilized a well-established method to chemically kill and metabolically inactivate the bacterial diet[25]. First, to study the effects of the diet on p38-MAPK activation, we employed the transgenic strain *Pcyp35B1::gfp*, where the promoter of a p38-MAPK-regulated CyTP gene (*cyp35B1*) drives the expression of *gfp*. This strain faithfully reports p38-MAPK activation in the *flr-4(-)* worms in response to B12[23,24]. We found that the increased CyTP gene expression observed in the *flr-4(-)* worms on a B12-rich diet was suppressed when HT115 or OP50 were treated with paraformaldehyde (PFA). The phenotype could not be restored when PFA-treated OP50 bacteria were exogenously supplemented with B12 (Supplementary Fig. S1D, E). Similar observations were made when the *flr-4(-)* worms were subjected to osmotic stress (Supplementary Fig. S1F,G). These results indicate that the increased CyTP gene expression and osmotic stress tolerance in *flr-4(-)* worms is attributed to B12 as well as the metabolite(s) produced by the metabolically active B12-rich bacteria.

B12 acts as a cofactor for the evolutionarily conserved MS (MTR, METR-1 in *C. elegans*) enzyme, facilitating the conversion of homocysteine to methionine (Fig. 1A). Targeted metabolomic analysis of *flr-4(-)* worms grown on both B12-rich diets- either OP50 supplemented with B12 or HT115, displayed a significantly increased levels of methionine compared to those of wild-type worms (Supplementary Fig. S1B, C)[24]. For the worms, the bacteria are the major source of this essential amino acid; it may be noted that the bacteria also require B12 for their Met-C to synthesize methionine. To ascertain whether the B12-rich diet also supplies methionine and remodels the Met-C in *flr-4(-)*, we exogenously supplemented OP50 with methionine. We observed that the diet rich in methionine was sufficient to increase the CyTP gene expression in *flr-4(-)* worms, similar to the worms when grown on OP50 supplemented with B12 (Supplementary Fig. S1H, I). However, the CyTP gene expression upon B12 or methionine supplementation required a functional host METR-1, as the *flr-4(-);metr-1(-)* worms failed to respond to these metabolites (Supplementary Fig. S3A, B). Together, these data suggest that a metabolically active bacterial diet rich in B12 or producing methionine may increase the flux through the host Met-C to promote longevity benefits in the *flr-4(-)* worms. These results also show that bacteria may supply both B12 as well as the essential amino acid methionine that influences the host Met-C and systemic physiology.

The *flr-4* expression is primarily confined to neuronal and intestinal cells, and knocking the gene down in either of these two tissues increased lifespan[23], CyTP gene expression (Supplementary Fig. S1J, K), as well as osmotolerance (Supplementary Fig. S1L). So, we asked in which specific tissue FLR-4 would interact with the Met-C to regulate downstream processes to ensure longevity. To discern this, we restored the expression of the *metr-1* cDNA selectively in either the neuronal cells of *flr-4(-);metr-1(-)*, using the pan-neuronal *rgef-1*

promoter [neu *metr-1(+)*], or intestinal cells, using the *ges-1* promoter [int *metr-1(+)*]. It may be noted that the increased CyTP gene expression, stress tolerance and lifespan of *flr-4(-)* is suppressed when *metr-1* is knocked down using RNAi[24] or knocked out using *metr-1* null mutant [*flr-4(-);metr-1(-)*] (Fig. 1B–E). We found that *flr-4(-);metr-1(-);Prgef-1::metr-1;Pcyp35B1::gfp* worms, when grown on HT115, where *metr-1* is rescued in the neuronal cells [neu *metr-1(+)*], exhibited increased expression of CyTP genes compared to control worms (Fig. 1B, C). However, *flr-4(-);metr-1(-);Pges-1::metr-1;Pcyp35B1::gfp* worms, where *metr-1* was rescued in the intestinal cells [int *metr-1(+)*], did not display enhanced GFP expression (Fig. 1B, C). Similarly, neuronal restoration of *metr-1* enhanced the osmotic stress tolerance (Fig. 1D) as well as the lifespan (Fig. 1E) of *flr-4(-);metr-1(-)* mutant worms to the level observed in *flr-4(-)*. Similar observations were made using a tissue-specific RNAi system (Supplementary Fig. S2A–C). We could attribute these benefits to the high B12 levels in HT115[24], as supplementing the OP50 with B12 could also restore the CyTP gene expression (Supplementary Fig. S2D, E) as well as osmotic stress tolerance (Supplementary Fig. S2F–H) only in the neuronally-expressed *metr-1* strain. Similarly, upon methionine supplementation, the CyTP gene expression was increased when *metr-1* was restored in the neurons of the *flr-4(-);metr-1(-)* worms (Supplementary Fig. S3A, B) Collectively, these observations provide evidence that the METR-1, and as a corollary Met-C, is crucial in the neurons, but not in the intestine, for the lifespan-extending phenotypic traits observed in the *flr-4(-)* worms grown on the B12-rich diet (Fig. 1F). It may be noted that in all these cases, the WT worms remained phenotypically unaffected by B12 or methionine supplementation, showing that FLR-4 helps to maintain adaptive capacity to a diet of high B12 or methionine content.

In our previous study, we found that the longevity benefits of *flr-4(-)* were dependent on the Kennedy pathway genes[24]. Dietary choline is converted to phosphatidylcholine (PC) through this pathway, and low PC is known to activate the p38-MAPK[24,26]. So, choline supplementation to the *flr-4(-)* worms on high B12 diet suppressed the longevity benefits mediated by p38-MAPK[24]. Now we asked whether choline supplementation would also affect the phenotypes of *flr-4(-)* dependent on the neuronal Met-C. For this, we supplemented choline to *flr-4(-);metr-1(-);Prgef-1::metr-1* worms grown on HT115 and found that the CyTP gene expression, osmotic stress tolerance and lifespan are suppressed (Supplementary Fig. S3C–F). This suggests that dietary choline can modify *flr-4(-)* phenotypes dependent on the neuronal Met-C.

p38-MAPK signaling in the intestine activates CyTP gene expression, and increases osmotic stress tolerance and longevity of the *flr-4* mutant

The *flr-4(-)* worms, grown on a B12-rich diet, exhibit an increased lifespan and health span attributed to the activation of the p38-MAPK pathway[23,24]. In *C. elegans*, this pathway acts as a central signaling mediator required for mounting an innate immune response when challenged with pathogens. The worm p38 ortholog PMK-1 is activated by its upstream MAPKKK NSY-1 and MAPKK SEK-1 (Fig. 2A)[27]. We aimed to delineate the specific tissue types where the NSY-1-SEK-1-PMK-1 signaling module is crucial for *flr-4(-)* to manifest the benefits. To accomplish this, we knocked down *pmk-1* only in the intestine using *flr-4(n2259);rde-1(ne219);Pnhx-2::rde-1* [intestine (int) only RNAi] and found that CyTP gene expression, osmotolerance and lifespan were completely suppressed (Supplementary Fig. S4A–D). However, these phenotypes remained unaffected in *flr-4(n2259);sid-1(pk3321);Punc-119::sid-1* [neuron (neu) only RNAi] worms (Supplementary Fig. S4A–D).

Since SEK-1 is the upstream kinase that phosphorylates PMK-1/p38-MAPK, we knocked this gene down using the same tissue-specific RNAi system mentioned above. We found that knocking down *sek-1* only in the intestine suppressed CyTP gene expression while neuron-specific knockdown had no effects (Fig. 2B, C). To further validate the involvement of intestinal SEK-1, we generated an *flr-4(-);sek-1(-);Pges-1::sek-1* strain that has *sek-1* cDNA expressed only in the intestinal cells [int *sek-1(+)*] and *flr-4(-);sek-1(-);Punc-119::sek-1* strain that expresses *sek-1* only in the neuronal cells [neu *sek-1(+)*]. We found that only the intestinal restoration of *sek-1* activated PMK-1/p38-MAPK as determined by western blot analysis (Supplementary Fig. S4E), enhanced the osmotic stress tolerance (Fig. 2D) as well as the longevity (Fig. 2E) of *flr-4(-);sek-1(-)* worms to the levels observed in *flr-4(-)* worms. Collectively, these observations provide evidence that the p38-MAPK pathway is required in the intestine for the phenotypic traits observed in the *flr-4(-)* worms (Fig. 2F).

The CyTP gene expression, osmotic stress tolerance and longevity of the *flr-4* mutant require serotonergic neurotransmission

Since the Met-C in the neurons and the p38-MAPK pathway in the intestine govern CyTP gene expression, osmotic stress tolerance, and longevity phenotypes in the *flr-4(-)* worms, we investigated how this inter-tissue communication is established (Fig. 3A). The dense core vesicles are required for neuropeptide release, while the clear synaptic vesicles are involved in neurotransmitter release. We used *flr-4(-);Pcyp31B1::gfp* worms and knocked down the representative genes required for neurotransmitter release (*unc-13*) or neuropeptide release (*unc-31*)[28,29] using RNAi. Interestingly, we observed that the increased CyTP gene expression in either scenario was diminished, suggesting that *flr-4(-)* engages certain downstream neuropeptides or neurotransmitters (Supplementary Fig. S4F, G). To identify the neurotransmitters, we systemically knocked down genes involved in dopamine (*cat-2*), glutamate (*eat-4*), octopamine (*tbh-1*), tyramine (*tdc-1*), serotonin (*tph-1*), acetylcholine (*unc-17*), or GABA (*unc-25*) biosynthesis in the *flr-4(-);Pcyp31B1::gfp* using RNAi. We found that the expression of *gfp* was suppressed on knocking down *tph-1* and *cat-2*, highlighting the importance of serotonergic and dopaminergic neurotransmission, respectively, in the *flr-4(-)* phenotype (Supplementary Fig. S4H). For further characterization of the *flr-4(-)* signaling cascade, in this study, we only report the involvement of the serotonergic arm.

We validated the involvement of serotonergic signaling in *flr-4(-)* phenotypes using a genetic deletion of *tph-1* gene (codes for tryptophan hydroxylase, the enzyme that catalyzes the first step and rate limiting step of serotonin biosynthesis) as in *flr-4(-);tph-1(-);Pcyp-35B1::gfp*; the expression of the CyTP reporter was suppressed (Fig. 3B, C). We also found that the increased lifespan of *flr-4(-)* is completely suppressed by *tph-1* deletion (Fig. 3D). A recent study has established the role of phenylalanine hydroxylase (*pah-1)* in the biosynthesis of non-neuronal 5-HT[30]. So, to further investigate serotonergic neurotransmission, we first determined whether non-neuronal 5-HT was also involved. For this, we knocked down *pah-1* and found that this did not affect the expression of *gfp* in *flr-4(-);Pcyp35B1::gfp*, pointing to the specific involvement of the neuronally synthesized 5-HT in *flr-4(-)* phenotype (Supplementary Fig. S5A, B). To confirm the role of 5-HT, we supplemented the neurotransmitter to the *flr-4(-);tph-1(-);Pcyp-35B1::gfp* worms where the *gfp* expression is suppressed due to the lack of serotonergic signaling. We found that the expression of *gfp* was restored (Fig. 3E, F). However, supplementation of 5-HT to the *Pcyp-35B1::gfp* and *flr-4(-);Pcyp-35B1::gfp* worms did not affect the CyTP gene expression (Supplementary Fig. S5C). Using a *tph-1::gfp* transgenic line, we found that the expression of the *tph-1* gene was transcriptionally upregulated in the serotonergic (ADF) neurons of the *flr-4(-)* grown on high-B12 diet (Supplementary Fig. S5D, E). Finally, using immunofluorescence, we show that the *flr-4(-)* grown on a high B12 diet has increased levels of serotonin in the serotonergic neurons (Fig. 3G, H). Together, these data suggest that in the *flr-4(-)* grown on high B12 diet, the engagement of the Met-C leads to an increase in serotonin biosynthesis through the transcriptional upregulation of the rate-limiting *tph-1* gene.

Serotonin is biosynthesized from the essential amino acid tryptophan (Trp). Beyond its role in protein synthesis and serotonin

https://doi.org/10.1038/s41467-025-60475-0

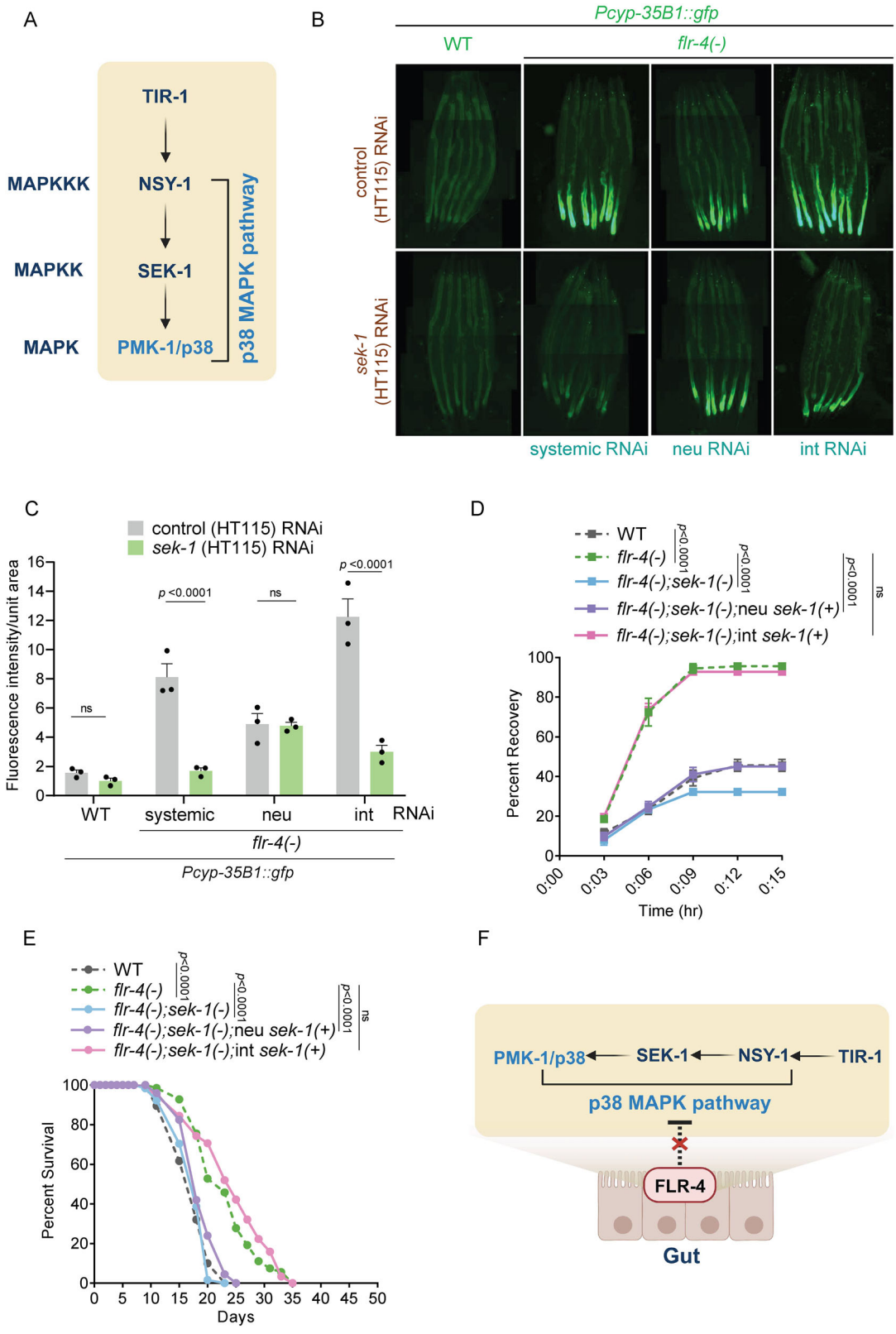

production, most Trp is degraded by the Kynurenine (Kyn) pathway to produce Kynurenic acid (KynA). Kyn synthesis is initiated by the rate-limiting enzyme tryptophan 2,3-dioxygenase (*tdo-2*), which is expressed in the peripheral tissues. Kyn is then transported to neurons by the transporter AAT-1, where it is acted upon by kynurenine aminotransferase (*nkat-1*) to form kynurenic acid (KynA). Alterations in KynA levels play a distinctive role in cognitive functions, learning and memory. KynA production acts as a neuroinhibitory metabolite of serotonin signaling[31–33]. Animal and clinical studies also show a relationship between B12 levels and Kyn pathway[34–36]. Given that *flr-4(-)* worms exhibit longevity benefits through serotonergic signaling, we investigated whether the Kyn pathway is involved in this phenotype. We knocked down the genes encoding the enzymes *tdo-2* and *nkat-1* and observed that the CyTP gene expression in both wild-type and

Fig. 2 | p38-MAPK pathway in the intestine modulates CyTP gene expression, osmotic stress tolerance and lifespan of *flr-4(n2259)*. **A** A schematic representation of the p38-MAPK pathway in *C. elegans*. Created in BioRender. Mukhopadhyay, A. (2025) https://BioRender.com/83r2ngb. **B** The expression of *gfp* was suppressed when *sek-1* was knocked down in *flr-4(n2259);rde-1(ne219);Pnhx-2::rde-1;Pcyp35B1::gfp* [intestine only RNAi (int RNAi)] but not in *flr-4(n2259);sid-1(pk3321);Punc-119::sid-1;Pcyp35B1::gfp* [neuron only RNAi (neu RNAi)] worms. One of three biologically independent replicates is shown. **C** Quantification of (**B**). Average of three biological replicates ± SEM. *P*-value determined using Two-way ANOVA with Tukey's Multiple Comparison Test. $P \geq 0.05$ was considered not significant, ns. **D** The osmotic stress tolerance was restored when *sek-1* was rescued only in the intestine of the *flr-4(n2259);sek-1(km4)* worms (using the *ges-1* promoter) [int *sek-1(+)*] but not when rescued in the neurons (using the pan-neuronal *unc-119* promoter) [neu *sek-1(+)*]. One of three biologically independent replicates is shown. *P*-value was determined using Two-way ANOVA with Tukey's multiple comparisons test. $P \geq 0.05$ was considered not significant, ns. **E** The lifespan was restored when *sek-1* was rescued only in the intestine of the *flr-4(n2259);sek-1(km4)* worms (using the *ges-1* promoter) [int *sek-1(+)*] but not when rescued in the neurons (using the pan-neuronal *unc-119* promoter) [neu *sek-1(+)*]. One of three biologically independent replicates shown. *P*-value was determined using Mantel–Cox log-rank test. $P \geq 0.05$ was considered not significant, ns. **F** A schematic illustrating that the p38-MAPK pathway is required in the gut. Created in BioRender. Mukhopadhyay, A. (2025) https://BioRender.com/83r2ngb. All experiments were performed at 20 °C. All data and analysis are provided in the Source Data file.

flr-4(-) worms remained unaffected (Supplementary Fig. S5F, G). Interestingly, however, exogenous supplementation of *flr-4(-)* worms with KynA suppressed CyTP gene expression (Supplementary Fig. S5H, I) and osmotic stress tolerance (Supplementary Fig. S5J) but did not affect wild-type worms. These findings suggest that *flr-4(-)* worms achieve longevity benefits probably by lowering the KynA levels, which could in turn enhance serotonin synthesis. This angle will need to be investigated in more detail in future to understand the extent of the regulation and determine how metabolic signals from the gut may affect neuronal functions of the *flr-4(-)* worms.

5-HT functions by binding to its cognate receptor at the post-synaptic neurons. To identify the 5-HT receptors that act downstream of FLR-4, we made double mutants of *flr-4(-);Pcyp-35B1::gfp* with each of the four receptor mutants, i.e., *ser-1(-)*, *ser-4(-)*, *ser-7(-)*, and *mod-1(-)*[37]. We found that *mod-1* mutation significantly suppressed the CyTP gene expression of the *flr-4(-);Pcyp-35B1::gfp* worms (Supplementary Fig. S5K, L) along with their osmotic stress tolerance (Supplementary Fig. S5M) and longevity (Supplementary Fig. S5N). Importantly, supplementing 5-HT to *flr-4(-);mod-1(-);Pcyp35B1::gfp* failed to increase *gfp* expression (Fig. 3I–K), suggesting that MOD-1 is the cognate receptor of 5-HT essential for downstream effects of *flr-4(-)*.

Serotonergic neurotransmission connects neuronal Met-C to the intestinal p38-MAPK pathway

Till now, we have only provided evidence of the requirement of serotonergic neurotransmission downstream of FLR-4. So next, to determine the hierarchy of the serotonergic neurotransmission in the Met-C-p38-MAPK cascade downstream of FLR-4, we used supplementation assays. First, we supplemented 5-HT to *flr-4(-);metr-1(-);Pcyp35B1::gfp* worms, where *gfp* fluorescence is low, and found that the expression was restored (Fig. 4A, B). Similarly, supplementation of 5-HT to *flr-4(-);metr-1(-)* worms increased the osmotic stress tolerance to the extent seen in *flr-4(-)* worms (Supplementary Fig. S6A). These show that serotonergic signaling works downstream of Met-C.

To ascertain the adequacy of rescuing the Met-C exclusively within the serotonergic neurons (ser neu) of *flr-4(-)* worms for the faithful recapitulation of the observed phenotypes, we transgenically rescued the *metr-1* cDNA using the *tph-1* promoter. Interestingly, we observed that reconstituting the Met-C specifically within the serotonergic neurons, using the *tph-1* promoter to drive expression of *metr-1*, was sufficient to increase the CyTP gene expression to the levels similar to worms where the pan-neuronal *rgef-1* promoter was used (Fig. 4C, D) and enhance the osmotic stress tolerance (Supplementary Fig. S6C) and lifespan (Supplementary Fig. S6D) of the *flr-4(-);metr-1(-)* worms.

Next, we identified the particular serotonergic neurons involved in modulating the Met-C. *C. elegans* has three pairs of serotonergic neurons; the chemosensory ADF neurons that perceive external environmental signals[38–40], the pharyngeal secretory NSM neurons that respond to food stimuli[41] and the egg-laying HSN motor neurons responsible for vulval contraction[42]. We rescued *metr-1* cDNA within the ADF neurons (using the *srh-142* promoter), the NSM neuron (using the *tph-1* short promoter), and within the HSN neurons (using the *egl-6* promoter)[41,43]. Met-C restoration specifically in the ADF neurons was sufficient to increase the CyTP gene expression (Fig. 4C, D, Supplementary Fig. S6B), osmotic stress tolerance (Supplementary Fig. S6C) and lifespan (Supplementary Fig. S6D) of the *flr-4(-);metr-1(-)* worms. Interestingly, supplementing methionine or B12 to OP50 could rescue the CyTP gene expression only when *metr-1* was made functional specifically in the serotonergic ADF neurons (Supplementary Fig. S3A, B). Collectively, these observations strongly indicate that Met-C, supported by B12 and methionine from the bacterial diet, exerts its influence within the ADF serotonergic neurons, leading to increased serotonergic neurotransmission.

Next, we asked whether FLR-4 exerts its influence on the Met-C in the ADF neurons cell autonomously. For this, when we rescued *flr-4* only in the ADF serotonergic neurons of *flr-4(-)* worms, it suppressed CyTP expression (Supplementary Fig. S6E, F) and osmotolerance (Supplementary Fig. S6G) to the levels observed when *flr-4* was rescued either pan-neuronally or in all serotonergic neurons, suggesting that the function of FLR-4 in the neurons is cell autonomous to modulate the Met-C.

While serotonergic signaling works downstream of the Met-C, it is also technically possible that this signaling may work downstream of the p38-MAPK. In that case, 5-HT supplementation should be independent of a functional p38-MAPK pathway. We tested this by supplementing 5-HT to the *flr-4(-);metr-1(-);Pcyp-35B1::gfp* worms grown on control or *sek-1* RNAi. We found that while the expression of *gfp* was restored on control RNAi, on *sek-1* RNAi, the expression failed to increase (Fig. 4E–G). Additionally, the increased osmotic stress tolerance observed in *flr-4(-);metr-1(-)* when supplemented with 5-HT, was not noticed in the *flr-4(-);sek-1(-)* worms (Supplementary Fig. S6H), proving that the p38-MAPK signaling works downstream of the serotonergic signaling.

Our data till now suggests that FLR-4 in the neurons prevent the Met-C-mediated activation of the serotonergic signaling. On the other hand, FLR-4 in the intestine may prevent ectopic activation of the p38-MAPK. If this is the case, the WT FLR-4 in the intestine should be able to prevent increased serotonergic signaling in the *flr-4(-)* worms from activating p38-MAPK in the intestine and provide osmotic stress tolerance. To test this scenario, we restored WT FLR-4 function only in the intestine of the *flr-4(-)* using the strain *flr-4(-);Pges-1::flr-4* and grew them on B12-rich HT115. We found that the CyTP gene expression (Supplementary Fig. S6E, F) and osmotic stress tolerance (Supplementary Fig. S6G) is suppressed. This experiment provides further evidence that FLR-4 functions to negatively regulate serotonergic signaling in the neurons as well as p38-MAPK activation in the intestine to maintain systemic homeostasis when the worms are fed bacteria of high B12 content (Fig. 4H).

FLR-2-FSHR-1 signaling functions downstream of the serotonergic signaling

While the serotonergic signaling connects the neuronal Met-C to intestinal p38-MAPK activation in the *flr-4(-)* worms, the 5-HT receptor

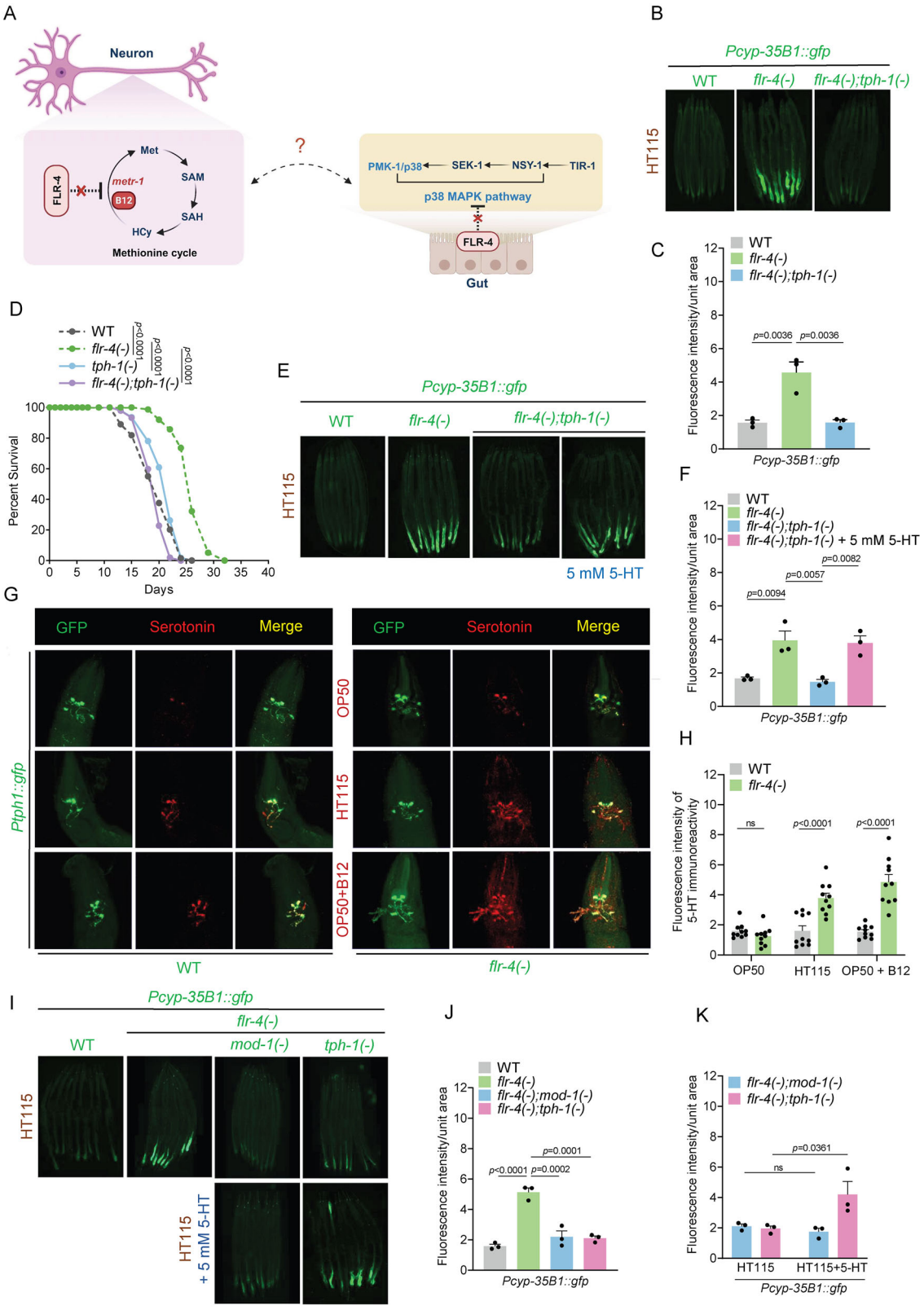

MOD-1 that we identified is expressed in the interneurons and not in the intestine[39,44,45]. In a screen aimed at identifying fluoride resistance (*flr*) genes, the *flr-4* was originally identified as one of the class 1 genes (*flr-1, flr-3* and *flr-4*). These mutants exhibited a strong temperature-sensitive defecation defect. The screen also identified the presence of the *flr-2*, which belongs to the class 2 *flr* genes (*flr-2, flr-5, flr-6* and *flr-7*), whose mutations suppress certain phenotypes associated with the class 1 genes[46–48]. FLR-2 is expressed in neurons and encodes a secreted protein that shares significant similarity with the human glycoprotein hormone subunit α2 of thyrostimulin[48,49]. So, we asked whether the neuropeptide FLR-2 could connect the signals from the MOD-1-expressing interneurons to the intestine.

In this direction, we had previously shown that knocking down *unc-31*, a gene which is involved in neuropeptide release from dense-

Fig. 3 | The activation of CyTP gene expression and longevity of *flr-4(n2259)* worms requires serotonergic signaling. A A schematic illustrating the potential inter-tissue crosstalk through a neuron-gut axis. Created in BioRender. Mukhopadhyay, A. (2025) https://BioRender.com/83r2ngb. **B** The expression of *gfp* was suppressed in case of *flr-4(n2259);tph-1(mg280);Pcyp35B1::gfp* worms compared to *flr-4(n2259);Pcyp35B1::gfp* worms. One of three biologically independent replicates is shown. **C** Quantification of (**B**). Average of three biological replicates ± SEM. *P*-value was determined using One-way ANOVA with Tukey's multiple comparisons test. $P \geq 0.05$ was considered not significant, ns. **D** The increased lifespan of *flr-4(n2259)* worms was suppressed when *tph-1* was mutated as in *flr-4(n2259);tph-1(mg280)*. One of three biologically independent replicates is shown. *P*-value was determined using Mantel–Cox log-rank test. $P \geq 0.05$ was considered not significant, ns. **E** The expression of *gfp* was restored when *flr-4(n2259);tph-1(mg280);Pcyp35B1::gfp* worms were supplemented with 5 mM 5-HT. One of three biologically independent replicates is shown. **F** Quantification of (**E**). Average of three biological replicates ± SEM. *P*-value determined using One-way ANOVA with Tukey's multiple comparisons test. $P \geq 0.05$ was considered not significant, ns. **G** The *flr-4(n2259);Ptph-1::gfp* worms, when grown on HT115 and on OP50 supplemented with 64 nM B12, showed increased serotonin immunoreactivity on immunofluorescence with anti-serotonin antibody. **H** Quantification of (**G**). Each data point represents fluorescence intensity of 5-HT immunoreactivity for one worm ($n = 10$). *P*-value determined using Two-way ANOVA with Tukey's multiple comparisons test. $P \geq 0.05$ was considered not significant, ns. **I** The expression of *gfp* in *flr-4(n2259);Pcyp35B1::gfp* worms was suppressed when *mod-1* was mutated as in *flr-4(n2259);mod-1(ok103);Pcyp35B1::gfp*. The supplementation of 5 mM 5-HT failed to restore *gfp* expression in *flr-4(n2259);mod-1(ok103);Pcyp35B1::gfp* but not in *flr-4(n2259);tph-1(mg280);Pcyp35B1::gfp* worms. One of three biologically independent replicates is shown. **J**, **K** Quantification of (**I**). Average of three biological replicates ± SEM. *P*-value determined using One-way ANOVA with Tukey's multiple comparisons test (**J**) and Two-way ANOVA with Tukey's multiple comparisons test (**K**). $P \geq 0.05$ was considered not significant, ns. All experiments were performed at 20 °C. All data and analysis are provided in the Source Data file.

core vesicles, suppresses the expression of *gfp* in *flr-4(-);Pcyp35B1::gfp* (Supplementary Fig. S4F,G). This prompted us to check the involvement of FLR-2 neuropeptide in modulating the *flr-4(-)* phenotype, connecting the MOD-1-containing interneuron to the intestine (Fig. 5A). We found that the *flr-2* mutation suppressed the *gfp* expression of *flr-4(-);Pcyp35B1::gfp* worms (Fig. 5B, C). Additionally, the osmotic stress tolerance (Fig. 5E) and the lifespan (Fig. 5G) of *flr-4(-)* worms were suppressed when *flr-2* was mutated. FLR-2 appears to function downstream of the 5-HT signaling, as 5-HT supplementation could not restore the expression of *gfp* in *flr-4(-);flr-2(-);Pcyp35B1::gfp* worms or the osmotic stress tolerance of the *flr-4(-);flr-2(-)* worms (Fig. 5B, D, F).

Having established that FLR-2 functions downstream of the serotonergic signaling, we then asked whether the neurons expressing MOD-1 are indeed the ones responsible for the release of FLR-2, thereby transducing signals from the serotonergic neurons to the intestine. Interestingly, upon transgenically expressing *flr-2* cDNA under the control of the *mod-1* promoter, we observed enhanced tolerance to osmotic stress (Fig. 5H), increased expression of the CyTP gene (Fig. 5I, J) and lifespan (Supplementary Fig. S7A). Thus, MOD-1-expressing neurons serve as the recipient for serotonergic signals and, in turn, release the neuropeptide FLR-2 for downstream activation of the p38-MAPK pathway in the intestine.

Next, we wanted to identify the cognate receptor for FLR-2 that transmits signals to the intestine. The intestinally-expressed FSHR-1 is a known receptor for FLR-2, facilitating signal transduction in response to cold-induced stress[50] and also to developmental cues[51]. To determine whether FSHR-1 also works downstream of the FLR-4 cascade, we visualized the expression of *gfp* in the *flr-4(-);fshr-1(-);Pcyp35B1::gfp* worms. We observed that the expression of *gfp* was reduced, showing that FSHR-1 functions in this pathway (Fig. 5B, C). Evidently, the osmotic stress tolerance (Fig. 5E) and the lifespan (Fig. 5G) of *flr-4(-)* worms were suppressed when *fshr-1* was mutated. Importantly, like FLR-2, FSHR-1 also acts downstream of the 5-HT signaling as 5-HT supplementation could not restore the expression of *gfp* (Fig. 5B, D) in *flr-4(-);fshr-1(-);Pcyp35B1::gfp* worms or the osmotic stress tolerance (Fig. 5F) of the *flr-4(-);fshr-1(-)* worms.

Next, we validated whether FSHR-1 is required in the intestine to support *flr-4(-)* phenotypes. For this, we specifically knocked down *fshr-1* in the intestine of the *flr-4(-);Pcyp35B1::gfp* or *flr-4(-)*, using an intestine-specific RNAi strain, which suppressed *gfp* expression (Supplementary Fig. S7B, C) and osmotic stress tolerance (Supplementary Fig. S7D), respectively. Importantly, systemic and intestinal knockdown, but not the neuronal knockdown, of *fshr-1* suppressed the long lifespan of *flr-4(-)* worms (Supplementary Fig. S7E). This shows that FLR-4-Met-C-serotonin-FLR-2 acts upstream of the intestinal FSHR-1 to activate the p38-MAPK signaling (Fig. 5K).

The Met-C-serotonin-FLR-2-FSHR-1 axis induces the TIR-1/SARM1 phase transition to activate the p38-MAPK pathway

Thus far, we have shown that the Met-C functions in the serotonergic neurons while the p38-MAPK works in the intestine of the *flr-4(-)* worms, connected by the serotonin-FLR-2/FSHR-1 axis. Next, we asked how the binding of FLR-2 to the intestinal FSHR-1 receptor activates the p38-MAPK pathway.

The TIR domain adapter protein TIR-1, an ortholog of human SARM1, acts upstream of the p38-MAPK pathway to modulate the expression of genes associated with immune responses[52,53]. The initiation of TIR-1 activation is prompted by a stress-induced phase transition, which facilitates protein oligomerization, augmenting NAD + glycohydrolase activity, and thereby activating the NSY-1/SEK-1/PMK-1 pathway[54]. So, we asked whether TIR-1/SARM1 phase transition is induced in the *flr-4(-)* worms to activate the p38-MAPK pathway. For this, we generated the *flr-4(-);tir-1::wrmScarlet* worms that reports TIR-1 expression[54] and observed a significant increase in the formation of visible puncta of the multimerized TIR-1::wrmScarlet protein within the intestinal epithelial cells of *flr-4(-)* worms, compared to the wild-type worms (Fig. 6A, B). Next, to investigate whether the Met-C-serotonin-FLR-2-FSHR-1 axis downstream of *flr-4* drives the phase transition of TIR-1/SARM1, we generated *flr-4(-);metr-1(-);tir-1::wrmScarlet, flr-4(-);tph-1(-);tir-1::wrmScarlet, flr-4(-);flr-2(-);tir-1::wrmScarlet* and *flr-4(-);fshr-1(-);tir-1::wrmScarlet*. As expected, abrogation of any of the components of the axis in the *flr-4(-)* worms significantly dampened the TIR-1 phase transition (Fig. 6B, Supplementary Fig. S8A). Thus, *flr-4(-)* worms induce TIR-1 oligomerization through the Met-C-serotonin-FLR-2-FSHR-1 axis, triggering the activation of the p38-MAPK pathway to ensure longevity (Fig. 6C).

Neuronal Met-C modulates foraging behavior through the serotonin-FLR-2-FSHR-1-p38-MAPK axis

Animals display food preferences or aversions based on environmental cues and nutritional requirements[55–57]. Previous studies have revealed that the worms can make dietary choices based on the nutritional quality of the food as well as their consequent effects on the survival trajectories[58–60]. Since the *flr-4(-)* worms benefit from the high B12 HT115 diet in terms of enhanced longevity, we asked whether these worms would be naturally inclined to choose HT115 over OP50. To determine this, wild-type and *flr-4(-)* worms were conditioned on either OP50 or HT115 (grown from L1 to L4 stage) and then allowed to choose between these two diets, kept on the opposite poles of a 100 mm plate (Fig. 7A). We observed that while the wild-type worms exhibited no preference towards HT115 diet, interestingly, the *flr-4(-)* worms conditioned on any diet consistently displayed a preference to these bacteria (Fig. 7B). Next, worms either conditioned on OP50 or OP50 supplemented with B12, were used for the food choice experiment. The *flr-4(-)* worms exhibited a preference towards

https://doi.org/10.1038/s41467-025-60475-0

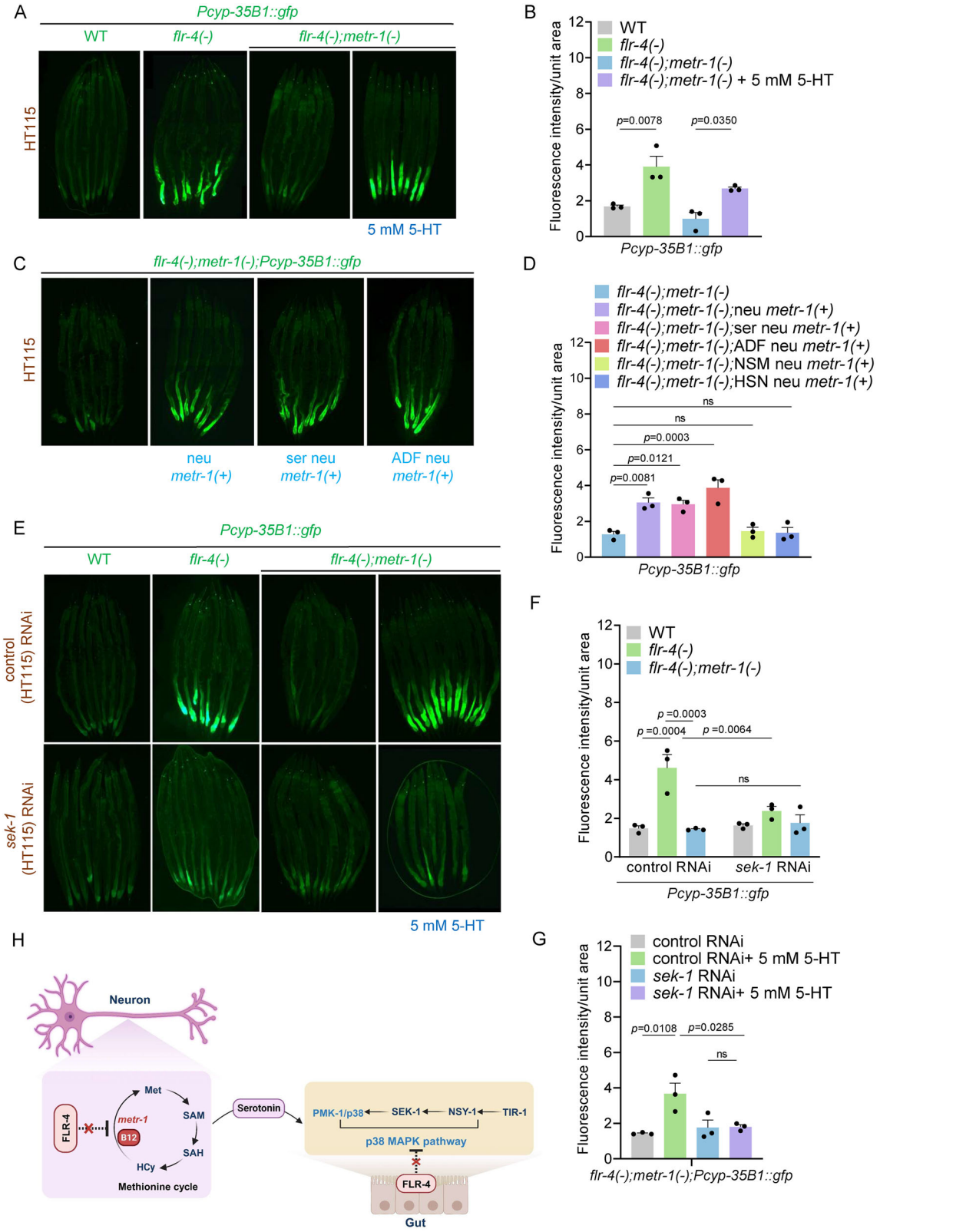

B12-supplemented OP50 diet, independent of preconditioning, suggesting that these worms were responding specifically to the high B12 levels of HT115 (Supplementary Fig. S9A).

Subsequently, we asked whether the foraging behavior towards the high B12 diet is also mediated by the reprogramming of the neuronal Met-C that activates the serotonin-FLR-2-FSHR-1-p38-MAPK axis. We observed that the preference of *flr-4(-)* worms towards HT115 is reversed when any of the components within the aforementioned cascade was mutated (Fig. 7C) while the preference of the wild-type worms remained unaffected (Supplementary Fig. S9B). Interestingly, rescuing the Met-C specifically within the ADF serotonergic neurons (but not in the HSN or NSM neurons) or the p38-MAPK pathway in the intestine (but not in the neurons) was sufficient for the preference of the *flr-4(-)* worms towards the HT115 diet (Fig. 7C). These experiments

Fig. 4 | Serotonergic neurotransmission connects the neuronal Met-C to the p38-MAPK pathway in the intestine. A The expression of *gfp* in *flr-4(n2259);metr-1(ok521);Pcyp35B1::gfp* worms was restored when these worms were supplemented with 5 mM 5-HT. One of three biologically independent replicates is shown. **B** Quantification of (**A**). Average of three biological replicates ± SEM. *P*-value determined using One-way ANOVA with Tukey's multiple comparisons test. $P \geq 0.05$ was considered not significant, ns. **C** The expression of *gfp* in *flr-4(n2259);metr-1(ok521);Pcyp35B1::gfp* worms was restored when *metr-1* was rescued pan-neuronally [ser neu *metr-1(+)*], only in the serotonergic neurons (using the *tph-1* promoter) [ser neu *metr-1(+)*] or in the ADF serotonergic neurons (using the *srh-142* promoter) [ADF neu *metr-1(+)*]. One of three biologically independent replicates is shown. **D** Quantification of (**C**) and (Supplementary Fig. S6B). Average of three biological replicates ± SEM. *P*-value determined using One-way ANOVA with Tukey's multiple comparisons test. $P \geq 0.05$ was considered not significant, ns. **E** The expression of *gfp* in *flr-4(n2259);metr-1(ok521);Pcyp35B1::gfp* worms failed to increase on supplementation with 5 mM 5-HT when *sek-1* was knocked down by RNAi. One of three biologically independent replicates is shown. **F**, **G** Quantification of (**E**). Average of three biological replicates ± SEM. *P*-value determined using Two-way ANOVA with Tukey's multiple comparisons test (**F**) and One-way ANOVA with Tukey's multiple comparisons test (**G**). $P \geq 0.05$ was considered not significant, ns. **H** A schematic illustrating the modulation of neuron-gut crosstalk through serotonergic signaling. Created in BioRender. Mukhopadhyay, A. (2025) https://BioRender.com/83r2ngb. All experiments were performed at 20 °C. All data and analysis are provided in the Source Data file.

suggest that the foraging behavioral of the *flr-4(-)* worms require the same neuron-gut signaling regulated by Met-C in the neurons to maximize longevity benefits associated with a diet rich in B12 levels.

Discussion

In this study, we elucidate an elegant neuron-gut axis that maintains normal life history traits in response to a diet having differential B12 content. B12 is required both by the bacterial as well as the host methionine synthase to drive their respective Met-C. The bacterial Met-C would also produce the essential amino acid methionine required for the worm Met-C. Our data suggest that in the kinase-dead *flr-4(-)* worms, the high B12 (and methionine) diet increases serotonin levels through the engagement of the Met-C in the ADF neurons. The WT FLR-4 kinase appears to prevent this process cell autonomously in the ADF neurons. The serotonin signaling in the *flr-4(-)* worms, through the MOD-1 receptor, leads to the release of FLR-2 neuropeptide from an interneuron that engages its cognate receptor in the intestine, FSHR-1. This signaling in the mutant leads to the activation of p38-MAPK through the oligomerization of TIR-1 in the intestine. Such activation is possible because, in the intestinal cells, the kinase-dead FLR-4 may fail to prevent TIR-1 oligomerization. Together, the FLR-4 kinase maintains adaptive capacity to the diet of high B12 content, thus helping in maintaining normal life history traits (Fig. 8).

Although the WT worms show accelerated development and increased fecundity on a high B12 diet, most other phenotypes that we and other groups have studied remain unaltered. For example, B12 or methionine supplementation does not affect lifespan in WT worms[61,62]. B12 also did not affect the acetylcholine release, reversal behavior, paralysis, speed, head bending, and body bends[63]. In all these cases, the effects of B12 supplementation were observed exclusively in the mutants, with no impact on WT worms[61–63]. In our study, the "adaptive capacity"[21,22] to different levels of dietary B12 is maintained by the *C. elegans* FLR-4 that prevents ectopic activation of the Met-C-mediated serotonergic signaling in the ADF neurons and inhibits the TIR-1 oligomerization in the intestine required for p38-MAPK activation; the dual regulatory roles of the kinase maintain normal life span on different bacterial diets. How the kinase achieves these regulations will be revealed once the phosphorylation targets are identified.

B12 is an important micronutrient; deficiency as well as excess has adverse effects on life history traits[17,26,64,65]. While deficiency lowers fertility, delays development, lowers pathogen resistance, and shortens lifespan, excess B12 in the diet can accelerate the growth rate, unnecessarily increase fecundity, and shorten lifespan[17,65]; all these changes may jeopardizes species' survival. This justifies the evolution of proteins like FLR-4 in nematodes to prevent abrupt changes in life history traits when the worms forage on a diet of differential nutritional content in their ecological niche. This gene also provides us with a unique paradigm to decipher how B12 influences a conserved metabolic pathway in the neurons to control the physiology of the entire body and regulate behavior and longevity. Since the bacteria are both the food as well as the microbiota of the worms, this simple paradigm also provides us with a genetically trackable model to study interspecies interactions that may be conserved in higher organisms.

The contribution of neurons in the regulation of longevity was recognized over two decades ago[66–68]. Neurons are responsible for detecting environmental cues as well as internal changes in energy balance to coordinate metabolic homeostasis[20]. The chemosensory neurons have earlier been shown to play an important role in modulating longevity[66]. Mutants that have impaired sensory cilia formation and, as a consequence, defective sensory perception, are often long-lived[68]. Even the increased lifespan by dietary restriction is mediated by the transcription factor SKN-1 acting only in the two ASI sensory neurons[69]. The thermosensory AFD neurons extend lifespan at warm temperatures by enhancing the DAF-9 sterol hormone signaling[70]. Interestingly, the chemosensory serotonergic ADF neurons are known to be activated by environmental cues and modulate food-dependent behaviors[71,72]. These pair of neurons are responsible for exhibiting learned aversive behaviors upon exposure to pathogenic bacteria by modulating immune responses[39,73]. Food-associated odors perceived by ADF neurons are responsible for regulating DR-dependent longevity[74]. However, the role of ADF neurons in modulating B12-driven behavioral and physiological responses has not been previously described. In our study, we have shown that exposure to metabolically active bacteria that supply both B12 and methionine at a higher level modulates the Met-C in the ADF neurons to alter gene expression, stress tolerance, longevity, and behavior.

Neuroendocrine signaling often directs the function of regulatory molecules in distal tissues such as the gut, to influence longevity. The cool-sensitive neurons IL1 extend lifespan through regulation of FOXO/DAF-16 function in the intestine at a lower temperature[75]. Neuronal FOXO/DAF-16 can communicate with the intestinal FOXO/DAF-16 to ensure longevity[76]. The AFD thermosensory neurons respond to warm temperatures by activating the HSF-1 transcription factor in the intestine using serotonin signaling[77]. Neuronal mitochondrial or ER proteotoxic stress signal is communicated to the intestine to mount an Unfolded Protein Response (UPR) that modulates longevity[78,79]. Consistent with the important role of neuron-gut signaling to modulate longevity, our findings exemplify how neurons process information related to the B12 content of food by modulating Met-C in the ADF neurons, transmitting them to downstream interneurons to modulate the p38-MAPK in the distal tissue, i.e., the intestine.

The gut microbiota employs multiple channels of communication to influence behavior and life-history traits of the host[80]. Bacterially-derived metabolites transmit signals to the nervous system, conveying information about the pathogenicity or commensalism[81]. The neuromodulator tyramine, produced by the *Providencia*, a commensal bacterium colonizing the gut, is converted to octopamine by the *C. elegans*, influencing the host's aversive sensory response[82]. The enteric serotonergic NSM neuron detects food ingestion via ion channels DEL-3 and DEL-7, which are localized to the sensory terminals of the enteric neuron in the gut and are required for the feeding-associated neuronal activation, which leads to slowing of the locomotion while the animal feeds[41]. Recently, B12-producing bacteria that colonize the gut have

https://doi.org/10.1038/s41467-025-60475-0

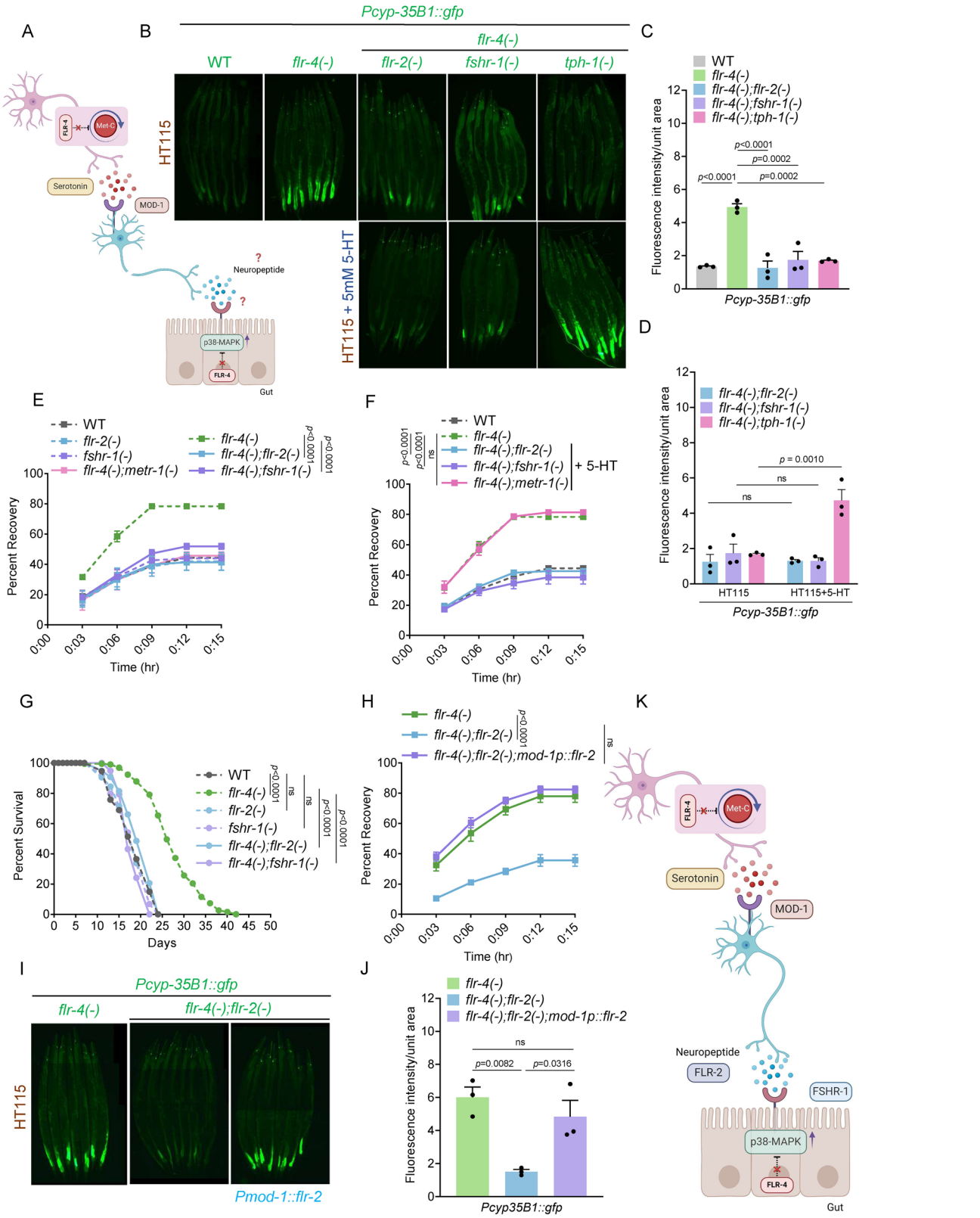

been shown to modulate neuronal excitatory cholinergic signaling and influence behavior[63]. Our study contributes to the growing understanding of host-microbiota interactions using *C. elegans* where the B12-rich gut microbiota can influence the nervous system to augment 5-HT biosynthesis. The Kyn pathway, which is fed by tryptophan from the bacterial diet, may influence this 5-HT signaling, further highlighting the role of the inter-species interaction. The serotonergic signaling, in turn, triggers downstream neuropeptide signaling, ultimately culminating in the activation of the p38-MAPK immune pathway within the intestinal milieu. The ensuing activation of the immune signaling pathway in the gut intricately modulates gene expression, stress tolerance, behavioral patterns, and, ultimately, longevity.

Distinct gut microbiota profiles are observed in depressed individuals compared to healthy controls[83]. Alterations in the composition

Fig. 5 | Involvement of the FLR-2-FSHR-1 axis in CyTP gene expression, osmotic stress tolerance, and lifespan of *flr-4(n2259)*. **A** A schematic showing the potential neuropeptide signaling axis downstream of the Met-C and serotonin. Created in BioRender. Mukhopadhyay, A. (2025) https://BioRender.com/83r2ngb. **B** The expression of *gfp* in *flr-4(n2259);Pcyp35B1::gfp* was suppressed when neuropeptide *flr-2* or its receptor *fshr-1* was mutated, as in *flr-4(n2259);flr-2(ut5);Pcyp35B1::gfp or flr-4(n2259);fshr-1(ok778);Pcyp35B1::gfp*, respectively. Additionally, supplementation with 5 mM 5-HT failed to restore the *gfp* expression in either strain, but could do so in the *flr-4(n2259);tph-1(mg280);Pcyp35B1::gfp* worms. One of three biologically independent replicates is shown. **C**, **D** Quantification of (**B**). Average of three biological replicates ± SEM. *P*-value determined using One-way ANOVA with Tukey's multiple comparisons test (**C**) and Two-way ANOVA with Tukey's multiple comparisons test (**D**). *P*-value determined using Two-way ANOVA with Tukey's multiple comparisons test. $P \geq 0.05$ was considered not significant, ns. **E** Osmotic stress tolerance of *flr-4(n2259)* was suppressed when *flr-2* or *fshr-1* was mutated, as in *flr-4(n2259);flr-2(ut5) or flr-4(n2259);fshr-1(ok778)*, respectively. One of three biologically independent replicates is shown. *P*-value was determined using Two-way ANOVA with Tukey's multiple comparisons test. **F** Supplementation of 5 mM 5-HT to *flr-4(n2259);flr-2(ut5)* or *flr-4(n2259);fshr-1(ok778)* failed to restore osmotic stress tolerance. One of three biologically independent replicates is shown. *P*-value was determined using Two-way ANOVA with Tukey's multiple comparisons test. *P*-value determined using Two-way ANOVA with Tukey's multiple comparisons test. $P \geq 0.05$ was considered not significant, ns. **G** The lifespan of *flr-4(n2259)* was suppressed when *flr-2* or *fshr-1* was mutated. One of two biologically independent replicates is shown. *P*-value was determined using Mantel–Cox log-rank test. *P*-value determined using Two-way ANOVA with Tukey's multiple comparisons test. $P \geq 0.05$ was considered not significant, ns. **H** Osmotic stress tolerance of *flr-4(n2259);flr-2(ut5)* worms was restored when *flr-2* cDNA was driven by the *mod-1* promoter as in *flr-4(n2259);flr-2(ut5);mod-1p::flr-2*. One of three biologically independent replicates is shown. *P*-value was determined using Two-way ANOVA with Tukey's multiple comparisons test. $P \geq 0.05$ was considered not significant, ns. **I** The expression of *gfp* in *flr-4(n2259);flr-2(ut5);Pcyp35B1::gfp* was restored when *flr-2* cDNA was driven by the *mod-1* promoter as in *flr-4(n2259);flr-2(ut5);mod-1p::flr-2;Pcyp35B1::gfp*. One of three biologically independent replicates is shown. **J** Quantification of (**I**). Average of three biological replicates ± SEM. *P*-value determined using One-way ANOVA with Tukey's multiple comparisons test. $P \geq 0.05$ was considered not significant, ns. **K** Model showing FLR-2 as the neuropeptide secreted by MOD-1 expressing interneuron and FSHR-1 as its intestinal receptor, downstream of the serotonergic signaling pathway in the *flr-4(-)* worms. Created in BioRender. Mukhopadhyay, A. (2025) https://BioRender.com/83r2ngb. All experiments were performed at 20 °C. All data and analysis are provided in the Source Data file.

of the human gut microbiota have been linked to mood disorders and neuropsychiatric conditions, with associated disruptions in neurotransmitter balance[84]. Discernible changes in the metabolic, immune, and endocrine systems also connect the pathophysiology of depression to the gut microbiota[85]. Individuals afflicted with psychotic illnesses frequently exhibit deficiencies in folate and B12, contributing to diminished levels of S-adenosylmethionine in the cerebrospinal fluid (CSF)[86]. To overcome this, patients are often co-administered with antidepressant drugs (like Selective Serotonin Reuptake Inhibitors; SSRIs) and B12 supplements[87,88], although the mechanistic underpinnings remain elusive. Like humans, worms are entirely dependent on diet or microbiota for B12 supply[1]. Although the neuronal network and general physiology of worms represent only a fraction of the complexity seen in mammals, our investigation provides a useful paradigm where one can study some of the mechanistic underpinnings of B12-mediated effects on serotonin signaling that affects behavior, which have to be validated later in higher systems. Complex interactions between B12 and cell signaling proteins like PP2a, p38 MAPK, MAPK/AKT, and SirT1-dependent ER stress response have been documented in mammalian brain and intestine[3,89,90]. In the future, it will be interesting to test whether these pathways play a role in the adaptive capacity to dietary differences in *C. elegans*.

Limitations of the study

While our study provides critical insights by which Met-C in a pair of serotonergic neurons regulates B12-dependent longevity through a neuron-gut signaling axis, some questions remain.

Conservation of the B12-driven neuron-gut signaling pathway in mammals. While many of the components of the neuron-gut signaling axis presented in this study are highly conserved, such as the Met-C, serotonin and the p38-MAPK pathway, others, like FLR-4, FLR-2 and FSHR-1, have weaker orthologs in mammals. So, in the future, it will be essential to reveal the functional conservation of this axis in mammals and identify core components. Using a genetically amenable model system, our study will prime the search for similar mechanisms used by higher mammals to adapt to changes in diet for maintaining a normal life span.

Identity of substrates of FLR-4. Our past[23,24], and present studies together suggest that *flr-4* has dual regulatory roles, one by regulating Met-C in the serotonergic neurons and the other by preventing ectopic activation of the p38-MAPK in the intestine. We have shown that both these tissue-intrinsic functions of the kinase are vital for transmitting the information of B12 differentials in diet to regulate life span and behavior. To fully understand how the kinase regulates the metabolic pathway in the neurons and the signal transduction pathway in the intestine, efforts need to be made to identify the substrates of FLR-4 phosphorylation in these two tissues.

Bacterial metabolites that influence the life span and behavior of the worms. Our findings suggest that FLR-4 kinase maintains homeostasis in the WT worms by preventing the ectopic activation of the p38-MAPK signaling pathway in the intestine, even when worms are exogenously supplied with B12 or methionine. While methionine has emerged as a key bacterial metabolite implicated in our study, apart from B12, it is likely that other microbiota-derived metabolites might also contribute to FLR-4-dependent neuron-gut signaling and longevity regulation. Identifying these metabolites and deciphering their functional interactions with the worm will be essential to gain a more comprehensive understanding of the gut-microbiota interaction.

Our study examines the interaction between the host and its microbiota using *C. elegans*, demonstrating that B12-rich gut microbiota can influence the nervous system to enhance 5-HT biosynthesis. The Kyn pathway, fed by tryptophan from the bacterial diet, may affect 5-HT signaling, further emphasizing the importance of inter-species interactions. We observed that exogenous supplementation of *flr-4(-)* worms with KynA suppressed CyTP gene expression and osmotic stress tolerance but did not impact wild-type worms. These observations suggest that *flr-4(-)* worms may achieve longevity benefits by reducing KynA levels, potentially boosting serotonin synthesis and activating the downstream intestinal p38-MAPK pathway through the neuron-gut signaling. Further investigation is needed to determine the extent of this regulation and how metabolic signals from the gut may influence neuronal functions in *flr-4(-)* worms.

The difference between *flr-4(n2259)* and *flr-4* RNAi phenotypes. While the *flr-4(n2259)* is obligately dependent on a high B12 diet for increased CyTP expression, osmotolerance and life span, the *flr-4* RNAi increased life span even in the low-B12 OP50 diet[23,24]. The *n2259* codes for a kinase-dead FLR-4 protein[91], while the RNAi leads to a reduction in the *flr-4* mRNA and possibly the levels of the kinase-proficient enzyme. Notably, the diet-dependent phenotypic differences are only associated with the kinase activity, as rescuing the kinase-dead mutant with a kinase-proficient FLR-4 rescues the life span on high B12 diet[23]. Although both interventions increase life span, the *flr-4* RNAi shows

https://doi.org/10.1038/s41467-025-60475-0

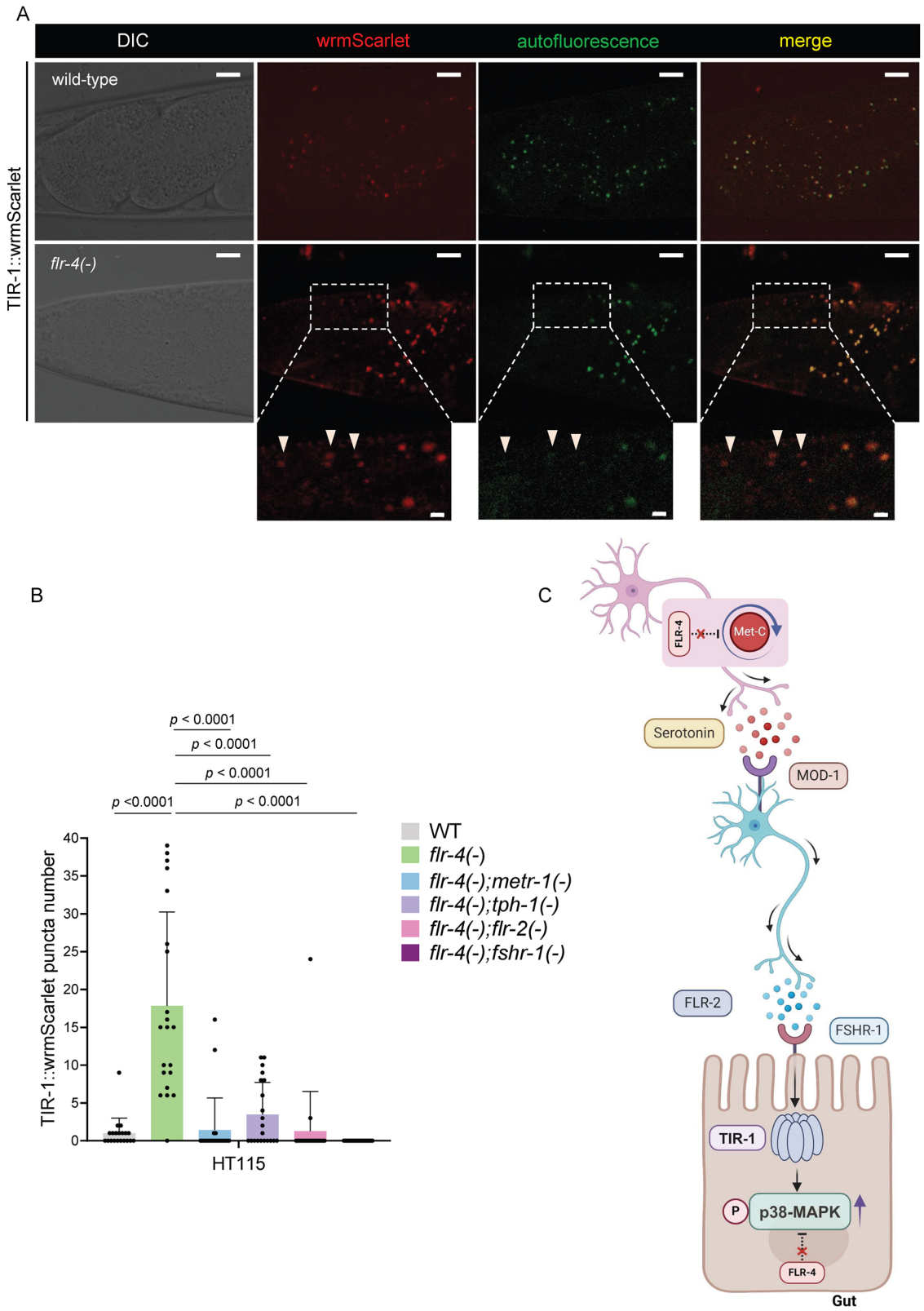

Fig. 6 | *flr-4(n2259)* worms induce SARM1/TIR-1 phase transition. A The *flr-4(n2259)* worms displayed increased TIR-1 puncta formation in comparison to wild-type worms. The red fluorescence channel images captured both TIR-1::wrmScarlet fluorescence and autofluorescence signals, while the green channel images exclusively revealed signals originating from the autofluorescent gut granules (Scale bar 10 µm). TIR-1::wrmScarlet puncta are denoted by arrowheads in the magnified images (Scale bar 2 µm). **B** Quantification of (**A**) and (Supplementary Fig. S8A). Each data point is the number of TIR-1::wrmScarlet puncta per worm. *P*-value determined using One-way ANOVA with Tukey's multiple comparisons test. **C** Model showing TIR-1 oligomerization leading to activation of the p38-MAPK pathway mediated by B12-rich diet in the *flr-4(n2259)* worms. Created in BioRender. Mukhopadhyay, A. (2025) https://BioRender.com/83r2ngb. All experiments were performed at 20 °C. All data and analysis are provided in the Source Data file. Created with BioRender.com.

https://doi.org/10.1038/s41467-025-60475-0

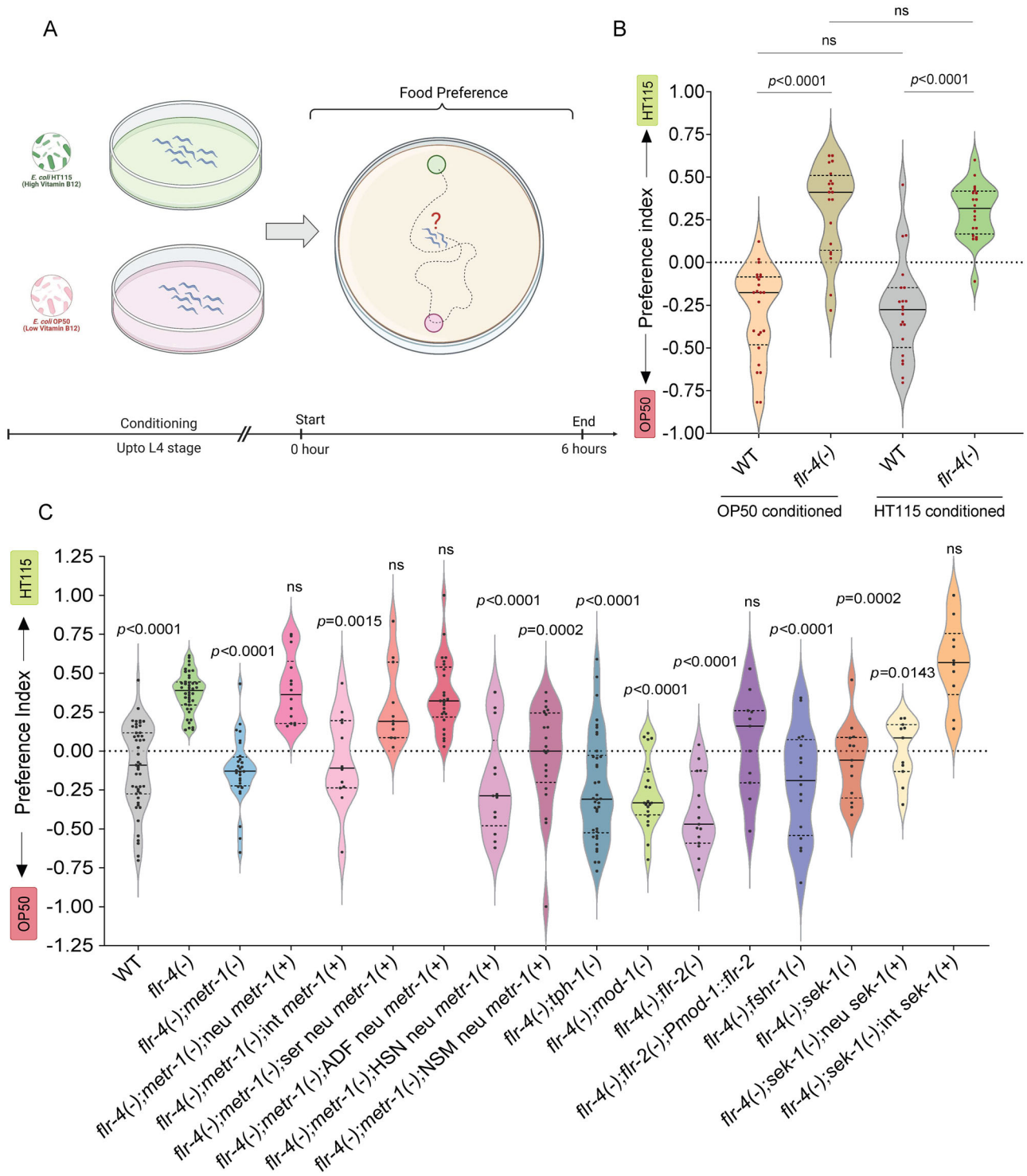

additional phenotypes like small body size and slow growth that are absent in the *n2259* worms (Supplementary Fig. S10G). We hypothesize that, among other possibilities, knocking down *flr-4* using RNAi may engage only the intestinal p38-MAPK, independent of the neuronal Met-C. In support of this, we found that both *flr-4* OP50 RNAi as well as *flr-4* HT115 RNAi increased CyTP and osmotolerance even in the *metr-1(-)* worms, whereas *flr-4(-);metr-1(-)* did not in either diet (Supplementary Fig. S10A–F). Also, while the transcriptome of *flr-4(n2259)* is enriched for genes of the Met-C, these genes were conspicuously missing in the transcriptome of the *flr-4* RNAi worms. However, CyTP gene expression was enriched in both interventions[23], suggesting that p38-MAPK signaling is engaged in both and may be the reason for the longevity benefits. We believe that the RNAi and the *n2259* engage distinct (Met-C-dependent or independent), yet some common signaling mechanisms. In further support of this inference, both *flr-4* OP50 RNAi and HT115 RNAi not only reduced the size of the *flr-4(n2259)* worms and slowed growth, but they also increased the CyTP gene expression and enhanced osmotic stress tolerance in a diet-independent manner (Supplementary Fig. S10G–I). Such differences in RNAi and mutant phenotypes have also been previously documented in the case of SGK-1[92,93], CLK-1[94,95] and CEP-1[96]. The different response/mechanism of the *flr-4* RNAi and *flr-4(n2259)* also suggests that domains other than the kinase domain of FLR-4 may have important biological functions that need to be deciphered in the

Fig. 7 | The *flr-4(n2259)* worms prefer the B12-rich HT115 diet. A A schematic representation of the food preference assay workflow. Created in BioRender. Mukhopadhyay, A. (2025) https://BioRender.com/83r2ngb. **B** The *flr-4(n2259)* worms, upon conditioning with either OP50 or HT115 diet, displayed a preference towards HT115, in contrast to wild-type worms, which showed no significant preference towards either diet. Each dot represents one plate with over 100 worms. All groups were tested on at least three independent trials, in three separate biological replicates. *P*-value determined using Kruskal–Wallis Test with Dunn's multiple comparisons test. $P \geq 0.05$ was considered not significant, ns. **C** The food preference of *flr-4(n2259)* worms towards HT115 diet was reversed when *metr-1, tph-1, mod-1, flr-2, fshr-1* or *sek-1* was mutated, as in *flr-4(n2259);metr-1(ok521), flr-4(n2259);tph-1(mg280), flr-4(n2259);mod-1(ok103), flr-4(n2259);flr-2(ut5), flr-4(n2259);fshr-1(ok778)* or *flr-4(n2259);sek-1(km4)*, respectively. Moreover, the rescue of *metr-1* in all neurons [neu *metr-1(+)*], serotonergic neurons [ser neu *metr-1(+)*] or ADF neurons [ADF neu *(metr-1(+)*], but not in HSN or NSM neurons of *flr-4(n2259);metr-1(ok521)* and intestinal rescue of *sek-1* [int *sek-1(+)*], but not the neuronal rescue, in *flr-4(n2259);sek-1(km4)* worms was sufficient to restore the altered food preference to that of *flr-4(n2259)* worms. Further, driving the expression of *flr-2* in the MOD-1 containing neurons rescued the food preference of *flr-4(n2259);flr-2(ut5)* worms. Each dot represents one plate with over 100 worms. All groups were tested on at least three independent trials, in three separate biological replicates. *P*-value determined using Kruskal–Wallis Test with Dunn's multiple comparisons test, in comparison with *flr-4(n2259)*. $P \geq 0.05$ was considered not significant, ns. All experiments were performed at 20 °C. All data and analysis are provided in the Source Data file.

future. Nonetheless, the *flr-4(n2259)* paradigm provided us with an opportunity to study B12-driven neuron-gut signaling that regulates longevity. The proposed model is based on the data generated using *flr-4(n2259)*.

Methods

Ethical statement

C. elegans is not subject to animal welfare regulations. The research conducted in this study complies with all ethical guidelines under the Institutional Bio-Safety Committee (IBSC) Approval # 384/20, issued by the National Institute of Immunology.

C. elegans growth and maintenance

All *C. elegans* strains were maintained at 20 °C on the Nematode Growth Medium (NGM) agar plates seeded with *Escherichia coli* OP50 bacteria as a food source for general maintenance. Depending upon the experiments, worms were either transferred to *E. coli* OP50 or *E. coli* HT115 seeded plates, post-L1 synchronization by bleaching. Transgenic animals were constructed by microinjection. The strains that were used and generated in this study are provided in Supplementary Data 1.

DNA constructs and generation of transgenics

For rescue constructs, the plasmid pNBRGWY32 (*Prgef-1::mbl-1*)[97] was used. This plasmid was subjected to linearization through PCR, strategically designed to exclude the *mbl-1*(cDNA). Required promoters were amplified from genomic DNA by PCR and cloned into it using the In-Fusion cloning methodology (In-Fusion® Snap Assembly Master Mix, #638947, Takara Bio). The PCR-amplified cDNA sequences: *metr-1*(cDNA), *flr-2* (cDNA) or *flr-4*(cDNA) were then fused with the linearized plasmid carrying their respective promoters, the pan-neuronal *Prgef-1*, intestinal *Pges-1*, serotonergic neuron-specific *Ptph-1*, ADF neuron-specific *Psrh-142*, HSN neuron-specific *Pegl-6*, NSM neuron specific *Ptph-1(short) or the Pmod-1* promoter as per the In-Fusion protocol. The construct (10–30 ng/µl) along with the co-injection marker *Pmyo-2::mCherry* (2 ng/µl) and L4440 empty vector (60–80 ng/µl) were injected into *flr-4(-);metr-1(-), flr-4(-);metr-1(-);Pcyp-35B1::gfp, flr-4(-);flr-2(-)* and *flr-4(-);flr-2(-);Pcyp-35B1::gfp, flr-4(-)* or *flr-4(-);Pcyp-35B1::gfp* worms. A list of all constructs generated for this study and primers used for the amplification can be found in Supplementary Data 2.

Bacterial growth

Bacteria stored in glycerol stocks were streaked onto Luria-Bertani (LB) plates and then allowed to incubate at 37 °C for 16 h until distinct single colonies became visible. A single colony was then used to inoculate LB broth and grown overnight at 37 °C for the primary culture. The secondary cultures were initiated with a 1/100th volume of the primary culture and left to incubate at 37 °C until the optical density (OD_{600}) of 0.6 was attained. The bacterial pellets were then resuspended in 1/10th volume of 1XM9 buffer. Approximately 300 µl of bacterial suspension was spread on NGM plates and left to dry for 1 day. The following bacterial strains were utilized: *E. coli* OP50 and *E. coli* HT115. The strains that were used in this study are provided in Supplementary Data 1.

RNA interference (RNAi) assay

The Ahringer or ORFeome *C. elegans* RNAi-feeding library was utilized for obtaining RNAi-feeding bacteria. The RNAi plasmids were verified for the correct target sequence. NGM RNAi plates were prepared by supplementing with 100 µg/ml ampicillin and 4 mM β-D-isothiogalactopyranoside (IPTG). RNAi bacteria were cultured overnight at 37 °C in LB media supplemented with 100 µg/ml ampicillin and 12.5 µg/ml tetracycline for the primary culture. The secondary cultures were initiated with a 1/100th volume of the primary culture supplemented with 100 µg/ml ampicillin and left to incubate at 37 °C until the OD_{600} of 0.6 was attained. The bacterial pellets were then resuspended in 1/10th volume of 1XM9 buffer, consisting of 100 µg/ml ampicillin and 1 mM IPTG. Approximately 300 µl of bacterial suspension was spread on NGM RNAi plates and left to dry for one day. Worms were exposed to RNAi plates from L1 onwards. Late L4 stage worms were transferred to freshly seeded RNAi plates to knock down genes expressed in the neurons.

Synchronization of worms

Gravid worms, cultivated on *E coli* OP50, were bleached, and the resulting eggs were exposed to L1 stage starvation for 16 h in 1XM9 buffer at 20 °C. Subsequently, the L1 larvae were subjected to centrifugation at 700 × *g* for one minute, followed by aspiration of the buffer. The L1 larvae were then transferred to the designated experimental plates.

Metabolite supplementation assay

A 3 mM stock solution of Vitamin B12 (#V6629; Sigma-Aldrich, USA) was prepared in double-distilled water. Subsequently, a working stock of 1 mM was prepared by diluting the 3 mM stock with 1XM9 buffer and then filtered. The 1 mM solution was then diluted to 64 nM with a 10-fold concentrated secondary bacterial culture and seeded on NGM plates.

A 300 mM stock of L-Methionine (#M9625; Sigma-Aldrich, USA) was dissolved in double-distilled water and filtered. The stock solution was then diluted to 10 mM with a 10-fold concentrated secondary bacterial culture and then seeded on NGM plates.

Choline chloride (#RC3917; G-Biosciences; USA) was freshly dissolved in double-distilled water at a concentration of 2 M and then filtered. The choline solution was added to autoclaved NGM at a final concentration of 40 mM choline-supplemented media plates, which were later seeded with bacterial feed.

A 100 mM stock of Serotonin hydrochloride (#H9523; Sigma-Aldrich, USA) was prepared in a 1XM9 buffer which was added to NGM plates seeded with bacteria to make a final plate concentration of 5 mM. Plates were allowed to dry for approximately 2 h.

A 50 mM stock solution of Kynurenic acid (#K3375; Sigma-Aldrich, USA) was dissolved in double-distilled which were added to NGM plates seeded with bacteria to make a final plate concentration of 0.625 mM, 1.25 mM or 2.5 mM. Plates were allowed to dry for approximately 2 h.

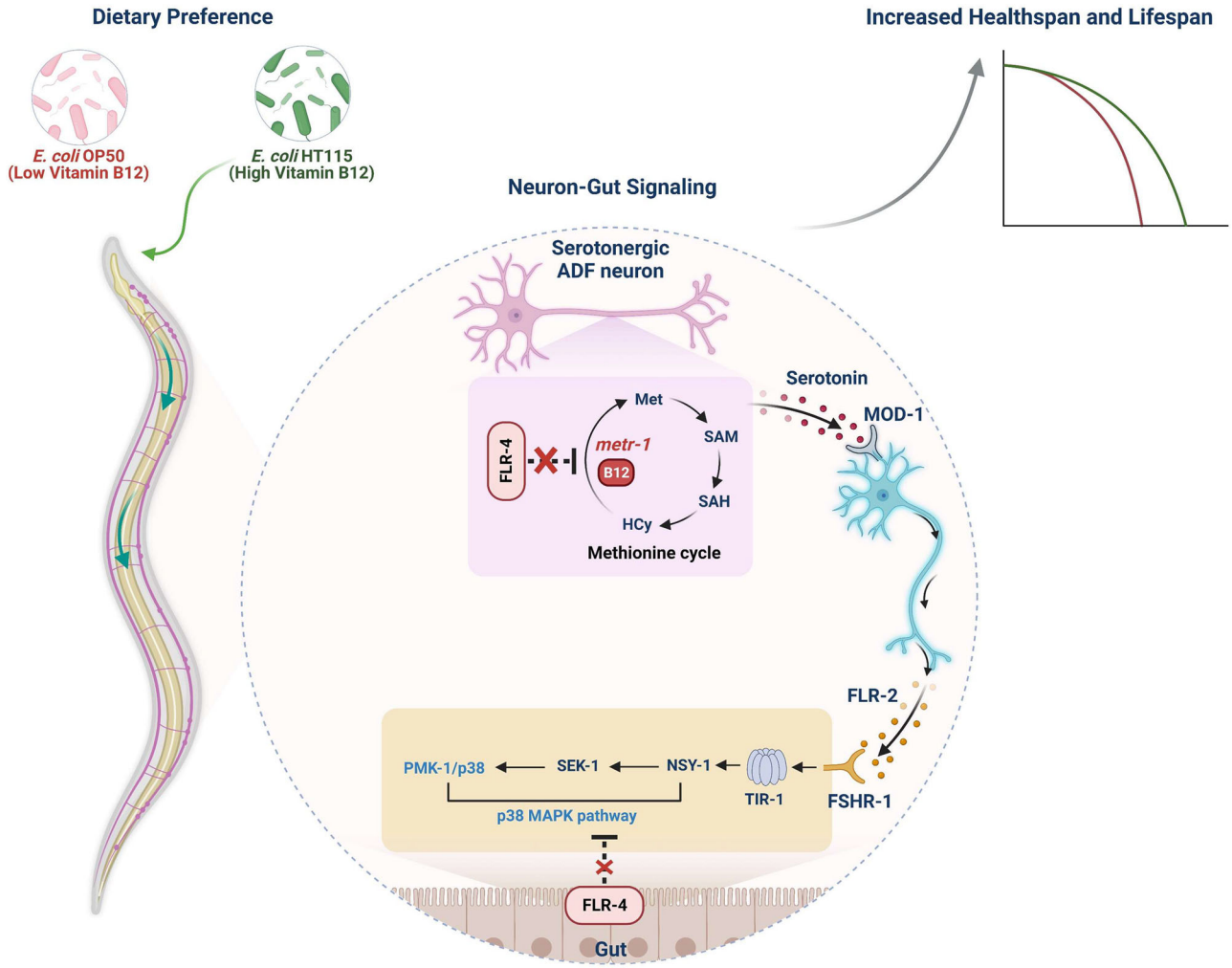

Fig. 8 | A model of the B12-dependent neuron-gut signaling axis regulated by FLR-4. A model delineating the possible mechanism by which *C. elegans* FLR-4 modulates longevity through a neuron-gut crosstalk, preventing aberrant activation of the Met-C and the p38-MAPK pathway on diet containing different B12 levels. In the *flr-4* mutant, grown on a high B12 diet, the flux through the Met-C localized in the ADF serotonergic neurons directs the release of serotonin, which binds to MOD-1, its cognate receptor in the interneurons. These interneurons, in turn, release the neuropeptide FLR-2, which then binds to its cognate receptor FSHR-1 in the intestine. This cascade induces the oligomerization of TIR-1, activating the downstream p38-MAPK pathway. Consequently, this leads to an increase in CyTP gene expression, enhancement of osmotic stress tolerance and an extension of the lifespan of the *flr-4* mutant grown on a high B12 diet. Created in BioRender. Mukhopadhyay, A. (2025) https://BioRender.com/83r2ngb.

Osmotic stress assay

The worms were raised on NGM plates containing 50 mM Sodium chloride (NaCl), seeded with the respective bacterial feeds (either supplemented or with RNAi). At the L4 stage, worms were then placed on unseeded NGM plates, which contained 350 mM NaCl, for 9 min. After this 9th minute, the worms were gently transferred onto unseeded NGM plates with 50 mM NaCl. The proportion of worms exhibiting movement was assessed over a 15-min timeframe to determine the percentage of recovery ($N = 3$, $n \geq 50$). For conducting statistical analyses on the recovery curve, *P*-values were determined by Two-way ANOVA using the GraphPad Prism 10 software.

Lifespan assay

L1 synchronized worms were grown on NGM plates seeded with the respective bacterial strains. Upon reaching the late L4 stage, the worms were transferred to plates overlaid with 5-fluorodeoxyuridine (FUDR; final concentration of 100 μg/ml). Lifespan assessment was started on the 7th day of adulthood and was continued every alternate day. Worms were scored as alive or dead by gently tapping with the platinum wire. *P*-values between survival curves were determined using the Log-rank (Mantel–Cox) test through OASIS 2 (Online application for survival analysis) software[98].

Food preference assay

Overnight-grown bacterial primary cultures were freshly inoculated in LB broth and were grown until an OD_{600} of 0.6 was attained at 37 °C. The bacterial pellets were then resuspended in 1/10th volume of 1XM9 buffer. Binary choice plates were made by seeding 10 μl of distinct bacterial suspensions at two opposite points on the 90 mm NGM assay plates, followed by an incubation period of 16 h at 20 °C. On the next day, L4-stage worms conditioned on specific bacterial diets or supplements were collected in 1XM9 buffer and washed thrice to remove bacteria. Approximately 100 worms were then placed into the center of the choice plate. After 6 h, the plates were examined and scored to observe the spatial distribution of the worms. The preference index (*I*) was calculated as $I = (N_{B12} - N_O)/(\text{Total number of worms})$, where N_{B12} is the number of worms in the B12-rich diet, i.e. either HT115 or OP50 supplemented with 64 nM B12, and N_O is the number of worms in the OP50 diet. A non-Gaussian distribution of residuals was assumed, so the non-parametric Kruskal–Wallis test, followed by Dunn's multiple comparisons test, was used to determine the *p*-value.

CyTP reporter imaging and analysis

For *Pcyp-35B1::gfp* expression visualization, all *Pcyp-35B1::gfp* expressing Day 1 adult worms, grown on either different diet, supplementation or RNAi, were mounted on 2% agarose-coated slides using 20 mM Sodium azide ($N = 3$, $n \geq 40$). The GFP fluorescence emitted by the worms was captured using an AxioImager M2 microscope (Carl Zeiss, Germany) at a magnification of 10X. Consistent exposure times, brightness, and contrast settings were maintained throughout the experiment. Individual images were stitched using Adobe Photoshop or Image J. GFP fluorescence was quantified by Fiji/ImageJ software[99] and subsequent statistical analyses were performed by using GraphPad Prism 10 software.

TIR-1::wrmScarlet puncta imaging and analysis

To visualize the expression of TIR-1::wrmScarlet, worms expressing TIR-1::wrmScarlet were subjected to *glo-3* RNAi from the L1 stage onwards, to deplete the autofluorescent gut granules[54]. For imaging, L4 stage worms were mounted on 2% agarose-coated slides using 20 mM Sodium azide. At 63 X, using the Zeiss LSM 980 Confocal Microscopy System, the posterior intestinal region was identified under the DIC channel. Images were then captured under the red channel to visualize the specific TIR-1::wrmScarlet puncta and the green channel to observe the autofluorescent gut granules. All images were acquired in Z-stacks, which were subsequently compressed into a single image. Quantification of TIR-1::wrmScarlet puncta was executed using the Fiji/ImageJ software[99], and subsequent statistical analyses were performed by using GraphPad Prism 10 software. The region of interest (ROI) was selected using the free-hand tool under the DIC channel. Subsequently, puncta in the red channel were identified using the Find Maxima tool, within the selected ROI. This information was then superimposed onto the green channel to identify the presence of autofluorescent puncta at the same spatial location. TIR-1::wrmScarlet puncta were considered as those exhibiting expression solely in the red channel and not in the green channel.

Immunofluorescence staining and analysis

Anti-serotonin staining was standardized following a previously published protocol[100]. Day 1 adult worms were fixed overnight at 4 °C in 4% paraformaldehyde prepared in PBS. The worms were washed with PBS containing 0.5% Triton X-100 (TrPBS) and then incubated for 14 h at 37 °C with shaking in 5% β-mercaptoethanol, 1% Triton X-100, and 100 mM Tris (pH 7.4). Worms were then washed in TrPBS and incubated for 45–90 min in a solution containing Collagenase type IV (C5138, Sigma-Aldrich) in 1 mM $CaCl_2$, 1% Triton X-100, and 100 mM Tris (pH 7.4). After another wash in TrPBS, samples were blocked for 1 h in 1% BSA in TrPBS. Worms were then incubated for 14–16 h at room temperature with the primary antibodies diluted in 1% BSA/TrPBS: anti-serotonin rabbit IgG (S5545, Sigma-Aldrich) and anti-GFP mouse IgG (Sc-9996, Santa Cruz Biotechnology). The next day, worms were rinsed 3 times throughout 1 h in 0.1% BSA/TrPBS and incubated with secondary antibodies diluted 1:100 in 1% BSA/TrPBS, including Alexa Fluor 488-conjugated goat anti-mouse IgG (115-545-003, Jackson ImmunoResearch) and Alexa Fluor 594-conjugated donkey anti-rabbit IgG (711-585-152, Jackson ImmunoResearch) for 4 h at 37 °C. Finally, the worms were rinsed once in TrPBS followed by 3–4 rinses in 0.1% BSA/TrPBS over 1 h before imaging. Imaging was performed at a magnification of 63X using the Zeiss LSM 980 Confocal Microscopy System. The localization patterns of serotonin were evaluated and quantified using the expression of *Ptph-1::gfp* to identify serotonergic neuronal cell bodies. All images were captured as Z-stacks and subsequently compressed into a single image. Consistent exposure times, brightness, and contrast settings were maintained throughout the experiment. The fluorescence intensity of serotonin immunoreactivity was quantified using the Fiji/ImageJ software. To eliminate the background staining, the area below the cell body in the same image was quantified and subtracted from the value obtained for the neuronal region.

Western blot assay

For each sample, 100 worms were picked in 1X M9 buffer, washed thrice and collected in 1X SDS Laemmli sample buffer. It was then boiled for 10 min and resolved by 10% SDS-PAGE. After complete electrophoretic separation, proteins were transferred to a nitrocellulose membrane. Following the transfer, the membrane was blocked with 5% BSA prepared in 0.1% TBST. The blots were then incubated overnight at 4 °C with either a phospho p38/PMK-1 antibody (1:1000, #9211, Cell Signaling Technology, USA) or an actin antibody (1:5000, #A5441, Sigma-Aldrich, USA) prepared in the blocking buffer. The next day, the blots were incubated for 1 h at room temperature with a secondary antibody (Abcam, #ab6721 and #AB6789) at a dilution of 1:10000 in 0.1% TBST. The blots were developed using an enhanced chemiluminescent substrate (Millipore, USA) and visualized in a ChemiDoc Imaging System (Azure Biosystems). Uncropped blots are provided in the Source Data.

Measuring intracellular vitamin B12 concentrations of *C. elegans*

Intracellular vitamin B12 levels were measured using a kit-based electrochemiluminescence immunoassay (ECLIA) on the COBAS e411 Analyzer. Briefly, young adult worm pellets from each experimental condition were collected into microcentrifuge tubes, washed three times with water, and gently pelleted. A freeze-dried pellet weighing 2.5 mg was resuspended in 75 µl of 1× PBS and homogenized with a handheld homogenizer. The homogenate was then centrifuged at 15,000 × *g* for 10 min at room temperature, after which the supernatant was collected for vitamin B12 quantification.

Metabolomics

Young Adult worms from each condition were collected in microcentrifuge tubes, washed three times with water, and gently pelleted. A 5 mg dry weight worm pellet was used for metabolite extraction. Intracellular metabolites for MS-based targeted metabolomics were extracted using pre-chilled Acetonitrile-methanol-water. For metabolite extraction, glass beads (#G8772, Sigma-Aldrich) were added. This was followed by quenching with chilled Acetonitrile-methanol-water (3:5:2) and vortexing for 30 s. The suspension was then centrifuged at 15,000 × *g* at 4 °C for 15 min. Supernatant was transferred to a fresh tube, vacuum dried and reconstituted in 25 µl of water with 0.1% formic acid. The reconstituted mixture was centrifuged at 15,000 x *g* for 10 min, and 5 µl was injected for LC–MS/MS analysis. The data were acquired using a UHPLC system coupled with a triple quadrupole mass spectrometer (TSQ Altis; Thermo) in a positive mode. Samples were loaded onto an Acquity UPLC BEH HILIC (1.7 µm, 2.1 × 100 mm) column, with a flow rate of 0.3 ml/min. The mobile phases comprised of water with 0.1% formic acid (buffer A) and acetonitrile with 0.1 % formic acid (buffer B). The linear mobile phase was applied from 95% to 20% of buffer A. The gradient program was used as follows: 95% buffer B for 1.5 min, 80%–50% buffer B in next 0.5 min, followed by 50% buffer B for next 2 min, and then decreased to 20% buffer B in next 50 s, 20% buffer B for next 2 min, and finally again 95% buffer B for next 4 min. Optimized ion source parameters were used, including ion spray voltage at 3500 V, sheath gas at 45 Arbitrary unit (AU), auxiliary gas at 10 AU, ion transfer tube temperature at 290 °C and vaporizer temperature was set to 300 °C. Multiple Reaction Monitoring (MRM) transitions used for quantification are added in Supplementary Data 3. The method cycle time was kept at 1 s. Data were acquired using five biological replicates. Relative quantification was performed using Skyline software. Data was exported in a CSV file, and fold change analysis was performed in MS Excel.

WormLab® image capture

Worm images were acquired using WormLab® software (MBF Bioscience) on 60 mm plates seeded with the respective bacterial feed. Photomicrographs were captured under standardized imaging conditions to ensure consistency across experimental replicates.

Quantification and statistical analysis

All statistical methods used in the manuscript are described in the figure legends, and additional details are provided in the method details. Statistics were computed using GraphPad Prism 10. Statistical tests used for each experiment are mentioned in the corresponding figure legend. All data and analysis are provided in the Source Data file. All illustrations were created using BioRender.com.

Reporting summary

Further information on research design is available in the Nature Portfolio Reporting Summary linked to this article.

Data availability

The authors declare that the main data supporting the findings of this study are available within the article and its supplementary files. The metabolomics data generated during this study have been deposited in the MetaboLights[101] database with identifier MTBLS12457, which can be directly accessed using the URL https://www.ebi.ac.uk/metabolights/reviewer5acc6c83-8af7-4a20-b770-6bc05a65c9d6. and also available upon request from the corresponding author. Source data are provided with this paper.

References

1. Watanabe, F. & Bito, T. Vitamin B (12) sources and microbial interaction. *Exp. Biol. Med.* **243**, 148–158 (2018).
2. Green, R. et al. Vitamin B(12) deficiency. *Nat. Rev. Dis. Prim.* **3**, 17040 (2017).
3. Gueant, J. L., Gueant-Rodriguez, R. M., Kosgei, V. J. & Coelho, D. Causes and consequences of impaired methionine synthase activity in acquired and inherited disorders of vitamin B(12) metabolism. *Crit. Rev. Biochem. Mol. Biol.* **57**, 133–155 (2022).
4. Parkhitko, A. A., Jouandin, P., Mohr, S. E. & Perrimon, N. Methionine metabolism and methyltransferases in the regulation of aging and lifespan extension across species. *Aging Cell* **18**, e13034 (2019).
5. Lionaki, E., Ploumi, C. & Tavernarakis, N. One-Carbon Metabolism: Pulling the Strings behind Aging and Neurodegeneration. *Cells* **11**, https://doi.org/10.3390/cells11020214 (2022).
6. Kennedy, K. P. et al. Vitamin B(12) supplementation in psychiatric practice. *Curr. Psychiatry Rep.* **26**, 265–272 (2024).
7. Raghubeer, S. & Matsha, T. E. Methylenetetrahydrofolate (MTHFR), the one-carbon cycle, and cardiovascular risks. *Nutrients* **13**, 4562 (2021).
8. Zarembska, E., Slusarczyk, K. & Wrzosek, M. The implication of a polymorphism in the methylenetetrahydrofolate reductase gene in homocysteine metabolism and related civilisation diseases. *Int. J. Mol. Sci.* **25**, 193 (2023).
9. Cortese, C. & Motti, C. MTHFR gene polymorphism, homocysteine and cardiovascular disease. *Public Health Nutr.* **4**, 493–497 (2001).
10. Petrone, I., Bernardo, P. S., Dos Santos, E. C. & Abdelhay, E. MTHFR C677T and A1298C polymorphisms in breast cancer, gliomas and gastric cancer: a review. *Genes* **12**, 587 (2021).
11. Newman, A. C. & Maddocks, O. D. K. One-carbon metabolism in cancer. *Br. J. Cancer* **116**, 1499–1504 (2017).
12. Pajares, M. A. & Perez-Sala, D. Betaine homocysteine S-methyltransferase: just a regulator of homocysteine metabolism?. *Cell Mol. Life Sci.* **63**, 2792–2803 (2006).
13. Wei, W. & Ruvkun, G. Lysosomal activity regulates Caenorhabditis elegans mitochondrial dynamics through vitamin B12 metabolism. *Proc. Natl Acad. Sci. USA* **117**, 19970–19981 (2020).
14. Giese, G. E. et al. Caenorhabditis elegans methionine/S-adenosylmethionine cycle activity is sensed and adjusted by a nuclear hormone receptor. *Elife* **9**, e60259 (2020).
15. Na, H., Ponomarova, O., Giese, G. E. & Walhout, A. J. M. C. elegans MRP-5 Exports Vitamin B12 from Mother to Offspring to Support Embryonic Development. *Cell Rep.* **22**, 3126–3133 (2018).
16. MacNeil, L. T., Watson, E., Arda, H. E., Zhu, L. J. & Walhout, A. J. Diet-induced developmental acceleration independent of TOR and insulin in C. elegans. *Cell* **153**, 240–252 (2013).
17. Yilmaz, L. S. & Walhout, A. J. Worms, bacteria, and micronutrients: an elegant model of our diet. *Trends Genet.* **30**, 496–503 (2014).
18. Van Pelt, K. M. & Truttmann, M. C. Caenorhabditis elegans as a model system for studying aging-associated neurodegenerative diseases. *Transl. Med. Aging* **4**, 60–72 (2020).
19. Miller, H. A., Dean, E. S., Pletcher, S. D. & Leiser, S. F. Cell non-autonomous regulation of health and longevity. *Elife* **9**, e62659 (2020).
20. Riera, C. E. & Dillin, A. Emerging Role of Sensory Perception in Aging and Metabolism. *Trends Endocrinol. Metab.* **27**, 294–303 (2016).
21. Nair, T. & Mukhopadhyay, A. Diet-gene interactions ensure optimal life span and health. *J. Biosci.* **48**, 42 (2023).
22. Yen, C. A. & Curran, S. P. Gene-diet interactions and aging in C. elegans. *Exp. Gerontol.* **86**, 106–112 (2016).
23. Verma, S., Jagtap, U., Goyala, A. & Mukhopadhyay, A. A novel gene-diet pair modulates C. elegans aging. *PLOS Genet.* **14**, e1007608 (2018).
24. Nair, T. et al. Adaptive capacity to dietary Vitamin B12 levels is maintained by a gene-diet interaction that ensures optimal life span. *Aging Cell* **21**, e13518 (2022).
25. Beydoun, S. et al. An alternative food source for metabolism and longevity studies in Caenorhabditis elegans. *Commun. Biol.* **4**, 258 (2021).
26. Ding, W. et al. s-Adenosylmethionine levels govern innate immunity through distinct methylation-dependent pathways. *Cell Metab.* **22**, 633–645 (2015).
27. Kim, D. H. et al. A conserved p38 MAP kinase pathway in Caenorhabditis elegans innate immunity. *Science* **297**, 623–626 (2002).
28. Brose, N., Rosenmund, C. & Rettig, J. Regulation of transmitter release by Unc-13 and its homologues. *Curr. Opin. Neurobiol.* **10**, 303–311 (2000).
29. Xu, T. & Xu, P. Searching for molecular players differentially involved in neurotransmitter and neuropeptide release. *Neurochem. Res.* **33**, 1915–1919 (2008).
30. Yu, J. et al. Parallel pathways for serotonin biosynthesis and metabolism in C. elegans. *Nat. Chem. Biol.* **19**, 141–150 (2023).
31. Schwarcz, R., Bruno, J. P., Muchowski, P. J. & Wu, H. Q. Kynurenines in the mammalian brain: when physiology meets pathology. *Nat. Rev. Neurosci.* **13**, 465–477 (2012).
32. Lemieux, G. A. et al. Kynurenic acid is a nutritional cue that enables behavioral plasticity. *Cell* **160**, 119–131 (2015).
33. Lin, L., Lemieux, G. A., Enogieru, O. J., Giacomini, K. M. & Ashrafi, K. Neural production of kynurenic acid in Caenorhabditis elegans requires the AAT-1 transporter. *Genes Dev.* **34**, 1033–1038 (2020).
34. Kretzschmar, G. C. et al. Folic acid and vitamin B12 prevent deleterious effects of rotenone on object novelty recognition memory and KYNU expression in an animal model of Parkinson's disease. *Genes* **13**, 2397 (2022).
35. Midttun, O. et al. Circulating concentrations of biomarkers and metabolites related to vitamin status, one-carbon and the kynurenine pathways in US, Nordic, Asian, and Australian populations. *Am. J. Clin. Nutr.* **105**, 1314–1326 (2017).
36. Khiroya, K., Sekyere, E., McEwen, B. & Bayes, J. Nutritional considerations in major depressive disorder: current evidence and

functional testing for clinical practice. *Nutr. Res. Rev.*, **38**, 25–36 (2023).
37. Carre-Pierrat, M. et al. Characterization of the Caenorhabditis elegans G protein-coupled serotonin receptors. *Invert. Neurosci.* **6**, 189–205 (2006).
38. Bargmann, C. I. & Horvitz, H. R. Control of larval development by chemosensory neurons in Caenorhabditis elegans. *Science* **251**, 1243–1246 (1991).
39. Zhang, Y., Lu, H. & Bargmann, C. I. Pathogenic bacteria induce aversive olfactory learning in Caenorhabditis elegans. *Nature* **438**, 179–184 (2005).
40. Song, B. M., Faumont, S., Lockery, S. & Avery, L. Recognition of familiar food activates feeding via an endocrine serotonin signal in Caenorhabditis elegans. *Elife* **2**, e00329 (2013).
41. Rhoades, J. L. et al. ASICs Mediate Food Responses in an Enteric Serotonergic Neuron that Controls Foraging Behaviors. *Cell* **176**, 85–97 e14 (2019).
42. Lloret-Fernandez, C. et al. A transcription factor collective defines the HSN serotonergic neuron regulatory landscape. *Elife* **7**, https://doi.org/10.7554/eLife.32785 (2018).
43. Flavell, S. W. et al. Serotonin and the neuropeptide PDF initiate and extend opposing behavioral states in C. elegans. *Cell* **154**, 1023–1035 (2013).
44. Churgin, M. A., McCloskey, R. J., Peters, E. & Fang-Yen, C. Antagonistic serotonergic and octopaminergic neural circuits mediate food-dependent locomotory behavior in Caenorhabditis elegans. *J. Neurosci.* **37**, 7811–7823 (2017).
45. Ranganathan, R., Cannon, S. C. & Horvitz, H. R. MOD-1 is a serotonin-gated chloride channel that modulates locomotory behaviour in C. elegans. *Nature* **408**, 470–475 (2000).
46. Katsura, I., Kondo, K., Amano, T., Ishihara, T. & Kawakami, M. Isolation, characterization and epistasis of fluoride-resistant mutants of Caenorhabditis elegans. *Genetics* **136**, 145–154 (1994).
47. Iwasaki, K., Liu, D. W. & Thomas, J. H. Genes that control a temperature-compensated ultradian clock in Caenorhabditis elegans. *Proc. Natl Acad. Sci. USA* **92**, 10317–10321 (1995).
48. Oishi, A. et al. FLR-2, the glycoprotein hormone alpha subunit, is involved in the neural control of intestinal functions in Caenorhabditis elegans. *Genes Cells* **14**, 1141–1154 (2009).
49. Park, J. I., Semyonov, J., Chang, C. L. & Hsu, S. Y. Conservation of the heterodimeric glycoprotein hormone subunit family proteins and the LGR signaling system from nematodes to humans. *Endocrine* **26**, 267–276 (2005).
50. Wang, C., Long, Y., Wang, B., Zhang, C. & Ma, D. K. GPCR signaling regulates severe stress-induced organismic death in Caenorhabditis elegans. *Aging Cell* **22**, e13735 (2023).
51. Torzone, S. K., Park, A. Y., Breen, P. C., Cohen, N. R. & Dowen, R. H. Opposing action of the FLR-2 glycoprotein hormone and DRL-1/FLR-4 MAP kinases balance p38-mediated growth and lipid homeostasis in C. elegans. *PLoS Biol.* **21**, e3002320 (2023).
52. Couillault, C. et al. TLR-independent control of innate immunity in Caenorhabditis elegans by the TIR domain adaptor protein TIR-1, an ortholog of human SARM. *Nat. Immunol.* **5**, 488–494 (2004).
53. Liberati, N. T. et al. Requirement for a conserved Toll/interleukin-1 resistance domain protein in the Caenorhabditis elegans immune response. *Proc. Natl Acad. Sci. USA* **101**, 6593–6598 (2004).
54. Peterson, N. D. et al. Pathogen infection and cholesterol deficiency activate the C. elegans p38 immune pathway through a TIR-1/SARM1 phase transition. *Elife* **11**, e74206 (2022).
55. Rainwater, A. & Guler, A. D. Food preference assay in male and female C57BL/6 mice. *J. Neurosci. Methods* **365**, 109384 (2022).
56. Anderson, G. H. & Li, E. T. Protein and amino acids in the regulation of quantitative and qualitative aspects of food intake. *Int J. Obes.* **11**, 97–108 (1987).
57. Johnson, A. W. Eating beyond metabolic need: how environmental cues influence feeding behavior. *Trends Neurosci.* **36**, 101–109 (2013).
58. Harris, G. et al. Dissecting the signaling mechanisms underlying recognition and preference of food odors. *J. Neurosci.* **34**, 9389–9403 (2014).
59. Abada, E. A. et al. C. elegans behavior of preference choice on bacterial food. *Mol. Cells* **28**, 209–213 (2009).
60. Shtonda, B. B. & Avery, L. Dietary choice behavior in Caenorhabditis elegans. *J. Exp. Biol.* **209**, 89–102 (2006).
61. Watson, E. et al. Interspecies systems biology uncovers metabolites affecting C. elegans gene expression and life history traits. *Cell* **156**, 759–770 (2014).
62. Amin, M. R., Mahmud, S. A., Dowgielewicz, J. L., Sapkota, M. & Pellegrino, M. W. A novel gene-diet interaction promotes organismal lifespan and host protection during infection via the mitochondrial UPR. *PLoS Genet.* **16**, e1009234 (2020).
63. Kang, W. K. et al. Vitamin B(12) produced by gut bacteria modulates cholinergic signalling. *Nat. Cell Biol.* **26**, 72–85 (2024).
64. Bito, T. & Watanabe, F. Biochemistry, function, and deficiency of vitamin B12 in Caenorhabditis elegans. *Exp. Biol. Med.* **241**, 1663–1668 (2016).
65. Macneil, L. T. & Walhout, A. J. Food, pathogen, signal: the multifaceted nature of a bacterial diet. *Worm* **2**, e26454 (2013).
66. Alcedo, J. & Kenyon, C. Regulation of C. elegans longevity by specific gustatory and olfactory neurons. *Neuron* **41**, 45–55 (2004).
67. Wolkow, C. A., Kimura, K. D., Lee, M. S. & Ruvkun, G. Regulation of C. elegans life-span by insulinlike signaling in the nervous system. *Science* **290**, 147–150 (2000).
68. Apfeld, J. & Kenyon, C. Regulation of lifespan by sensory perception in Caenorhabditis elegans. *Nature* **402**, 804–809 (1999).
69. Bishop, N. A. & Guarente, L. Genetic links between diet and lifespan: shared mechanisms from yeast to humans. *Nat. Rev. Genet.* **8**, 835–844 (2007).
70. Lee, S. J. & Kenyon, C. Regulation of the longevity response to temperature by thermosensory neurons in Caenorhabditis elegans. *Curr. Biol.* **19**, 715–722 (2009).
71. Sze, J. Y., Victor, M., Loer, C., Shi, Y. & Ruvkun, G. Food and metabolic signalling defects in a Caenorhabditis elegans serotonin-synthesis mutant. *Nature* **403**, 560–564 (2000).
72. Sawin, E. R., Ranganathan, R. & Horvitz, H. R. C. elegans locomotory rate is modulated by the environment through a dopaminergic pathway and by experience through a serotonergic pathway. *Neuron* **26**, 619–631 (2000).
73. Xie, Y., Moussaif, M., Choi, S., Xu, L. & Sze, J. Y. RFX transcription factor DAF-19 regulates 5-HT and innate immune responses to pathogenic bacteria in Caenorhabditis elegans. *PLoS Genet.* **9**, e1003324 (2013).
74. Zhang, B., Jun, H., Wu, J., Liu, J. & Xu, X. Z. S. Olfactory perception of food abundance regulates dietary restriction-mediated longevity via a brain-to-gut signal. *Nat. Aging* **1**, 255–268 (2021).
75. Zhang, B. et al. Brain-gut communications via distinct neuroendocrine signals bidirectionally regulate longevity in C. elegans. *Genes Dev.* **32**, 258–270 (2018).
76. Uno, M. et al. Neuronal DAF-16-to-intestinal DAF-16 communication underlies organismal lifespan extension in C. elegans. *iScience* **24**, 102706 (2021).
77. Tatum, M. C. et al. Neuronal serotonin release triggers the heat shock response in C. elegans in the absence of temperature increase. *Curr. Biol.* **25**, 163–174 (2015).
78. Berendzen, K. M. et al. Neuroendocrine coordination of mitochondrial stress signaling and proteostasis. *Cell* **166**, 1553–1563 e1510 (2016).

79. Taylor, R. C. & Dillin, A. XBP-1 is a cell-nonautonomous regulator of stress resistance and longevity. *Cell* **153**, 1435–1447 (2013).
80. Nagpal, J. & Cryan, J. F. Microbiota-brain interactions: moving toward mechanisms in model organisms. *Neuron* **109**, 3930–3953 (2021).
81. Meisel, J. D. & Kim, D. H. Behavioral avoidance of pathogenic bacteria by Caenorhabditis elegans. *Trends Immunol.* **35**, 465–470 (2014).
82. O'Donnell, M. P., Fox, B. W., Chao, P. H., Schroeder, F. C. & Sengupta, P. A neurotransmitter produced by gut bacteria modulates host sensory behaviour. *Nature* **583**, 415–420 (2020).
83. Liang, S., Wu, X. & Jin, F. Gut-brain psychology: rethinking psychology from the microbiota-gut-brain axis. *Front. Integr. Neurosci.* **12**, 33 (2018).
84. Huang, T. T. et al. Current understanding of gut microbiota in mood disorders: an update of human studies. *Front. Genet.* **10**, 98 (2019).
85. Caspani, G., Kennedy, S., Foster, J. A. & Swann, J. Gut microbial metabolites in depression: understanding the biochemical mechanisms. *Micro. Cell* **6**, 454–481 (2019).
86. Sharma, A. et al. S-Adenosylmethionine (SAMe) for neuropsychiatric disorders: a clinician-oriented review of research. *J. Clin. Psychiatry* **78**, e656–e667 (2017).
87. Syed, E. U., Wasay, M. & Awan, S. Vitamin B12 supplementation in treating major depressive disorder: a randomized controlled trial. *Open Neurol. J.* **7**, 44–48 (2013).
88. Coppen, A. & Bolander-Gouaille, C. Treatment of depression: time to consider folic acid and vitamin B12. *J. Psychopharmacol.* **19**, 59–65 (2005).
89. Melhem, H. et al. Methyl-deficient diet promotes colitis and SIRT1-mediated endoplasmic reticulum stress. *Gut* **65**, 595–606 (2016).
90. Chen, M. et al. Methyl deficient diet aggravates experimental colitis in rats. *J. Cell Mol. Med.* **15**, 2486–2497 (2011).
91. Take-uchi, M., Kobayashi, Y., Kimura, K. D., Ishihara, T. & Katsura, I. FLR-4, a novel serine/threonine protein kinase, regulates defecation rhythm in Caenorhabditis elegans. *Mol. Biol. Cell* **16**, 1355–1365 (2005).
92. Chen, A. T., Guo, C., Dumas, K. J., Ashrafi, K. & Hu, P. J. Effects of Caenorhabditis elegans sgk-1 mutations on lifespan, stress resistance, and DAF-16/FoxO regulation. *Aging Cell* **12**, 932–940 (2013).
93. Hertweck, M., Gobel, C. & Baumeister, R. C. elegans SGK-1 is the critical component in the Akt/PKB kinase complex to control stress response and life span. *Dev. Cell* **6**, 577–588 (2004).
94. Hamilton, B. et al. A systematic RNAi screen for longevity genes in C. elegans. *Genes Dev.* **19**, 1544–1555 (2005).
95. Lakowski, B. & Hekimi, S. Determination of life-span in *Caenorhabditis elegans* by four clock genes. *Science* **272**, 1010–1013 (1996).
96. Derry, W. B., Putzke, A. P. & Rothman, J. H. Caenorhabditis elegans p53: role in apoptosis, meiosis, and stress resistance. *Science* **294**, 591–595 (2001).
97. Puri, D. et al. Muscleblind-1 interacts with tubulin mRNAs to regulate the microtubule cytoskeleton in C. elegans mechanosensory neurons. *PLoS Genet.* **19**, e1010885 (2023).
98. Han, S. K. et al. OASIS 2: online application for survival analysis 2 with features for the analysis of maximal lifespan and healthspan in aging research. *Oncotarget* **7**, 56147–56152 (2016).
99. Schindelin, J. et al. Fiji: an open-source platform for biological-image analysis. *Nat. Methods* **9**, 676–682 (2012).
100. Loer, C. M. & Kenyon, C. J. Serotonin-deficient mutants and male mating behavior in the nematode Caenorhabditis elegans. *J. Neurosci.* **13**, 5407–5417 (1993).
101. Yurekten, O. et al. MetaboLights: open data repository for metabolomics. *Nucleic Acids Res.* **52**, D640–D646 (2024).

Acknowledgements

We thank the present and former members of the Molecular Aging Laboratory (National Institute of Immunology) for their support, Nafees Ansari for helping with the western blot assay and Prerona Ghosh for helping with molecular cloning. We are grateful to Dr. Anindya Ghosh Roy for his valuable suggestions and guidance, Drs. Manish Chamoli and Gautam Chandra Sarkar for the critical reading of the manuscript. We thank Dr. Read Pukkila-Worley (University of Massachusetts Chan Medical School) for generously providing the *C. elegans* strain RPW403 *tir-1(ums63[tir-1::wrmScarlet])*. Some strains were provided by the *Caenorhabditis* Genetics Center (CGC), which is funded by the National Institutes of Health (NIH) Office of Research Infrastructure Programs (P40 OD010440). This project was partly funded by the National Bioscience Award for Career Development (BT/HRD/NBA/38/04/2016), SERB-STAR award (STR/2019/000064), J.C. Bose Fellowship (JCB/2022/000021), SERB grant (CRG/2022/000525), DBT grant (BT/PR27603/GET/119/267/2018) to A.M., and core funding from the National Institute of Immunology.

Author contributions

A.M. and S.S.R. conceptualized the project. S.S.R., S.B., S.M., G.P and T.N. performed all the experiments except the metabolomics, which was performed by R.U. and S.C. under the supervision of S.S.G. S.S.R., S.B., S.M., and G.P. analyzed the data. S.S.R., S.B., G.P., and R.S.K. generated reagents for the project. A.M. and S.S.R. wrote the initial draft of the manuscript. A.M., S.S.R. and S.B. prepared the revised version of the manuscript. A.M. supervised the project and acquired funding.

Competing interests

The authors declare no competing interests.

Additional information

Supplementary information The online version contains supplementary material available at https://doi.org/10.1038/s41467-025-60475-0.

Correspondence and requests for materials should be addressed to Arnab Mukhopadhyay.

Peer review information *Nature Communications* thanks Ajay Bhat and the other anonymous reviewer(s) for their contribution to the peer review of this work. A peer review file is available.